






LGS steel shear wall system to retrofit or upgrade r.c. frame structures

Authors: Ludovic Fülöp

Confidentiality: Public

Report's title LGS steel shear wall system to retrofit or upgrade r.c. frame structures	
Customer, contact person, address Commission of the European Communities	Order reference RFS-PR-06054
Project name Steel Solutions for Seismic Retrofit and Upgrade of Existing Constructions	Project number/Short name 12597/STEELRETRO
Author(s) Ludovic Fulop	Pages 45 p.
Keywords concrete structure, pushover analysis, frame earthquake performance, retrofitting	Report identification code VTT-R-04770-09
Summary <p>This document is part of the project STEELRETRO, Work Package 3. One task of the work package was to evaluate the earthquake performance of a reinforced concrete building, and to propose rehabilitation and retrofitting solutions in order to improve it. The results of this task are reported in this document.</p> <p>The building under investigation was the "Reinforced concrete benchmark building" proposed within the STEELRETRO project. The main task here was to investigate potential retrofitting solutions based on the use of Light-Gauge Steel (LGS) elements.</p> <p>Finite Element Modelling of the building is carried out in this work, evaluating the earthquake performance using the pushover methodology. The proposed rehabilitation techniques are classified based on their technical performance. The final part of the document presents the performance improvement obtained using the LGS retrofitting in Performance Based Design format.</p>	
Confidentiality	Public
Espoo 18.1.2010	
Written by  Ludovic Fulop Senior Research Scientist	Reviewed by  Ilkka Hakola Senior Research Scientist
	Accepted by  Eila Lehmus Technology Manager
VTT's contact address P.O. Box 1000, FI-02044 VTT, Finland	
Distribution (customer and VTT) Customer (Partners of RFCS project STEELRETRO): 1 pdf copy VTT/Register Office: 1 copy	
<i>The use of the name of the VTT Technical Research Centre of Finland (VTT) in advertising or publication in part of this report is only permissible with written authorisation from the VTT Technical Research Centre of Finland.</i>	

Preface

The report is part of the project STEELRETRO, Work Package 3. The overall aim of the STEELRETRO project is to “*set up steel solutions for the seismic retrofit of existing buildings, furnishing design and construction methodologies, tools for dimensioning of elements and connections as well as for cost estimation*”.

Specifically, Work Package 3 aims at analyzing and designing “*steel solutions to retrofit or upgrade vertical systems of existing reinforced concrete building, in terms of strength or stiffness, by means of steel concentric bracing systems, steel eccentric bracing systems or shear steel/composite walls.*” and “*steel solutions to retrofit or upgrade vertical systems of existing masonry building coupling the existing structure with new a steel structure or with a bracing systems.*”

WP 3 also aims at analysis and design of “*steel solutions to retrofit or upgrade vertical systems of existing reinforced concrete building and masonry buildings, in terms of ductility by the application of dissipative steel systems and in particular by eccentric steel bracings, steel shear panels/walls and BRB (buckling restrained brace) systems.*”

Within WP 3, VTT had the role of analyzing “*possible solutions using light gauge steel shear walls*” for the r.c. frame structures; and light-gauge steel solutions both for the masonry building.

This report summarizes the work carried out for the rehabilitation of the reinforced concrete benchmark building.

Espoo 18.1.2010

Authors

Contents

Preface	2
Abbreviation and terminology	5
1 Introduction.....	6
2 FEM model development.....	6
3 Material models	8
3.1 Nominal material properties	8
3.2 Modeling of cross-sections.....	9
3.3 Performance criteria.....	9
4 Loads on the structure.....	10
4.1 Loads other than the frame elements ($/m^2$).....	10
4.2 Total loads/floor level other than the frame elements	10
4.2.1 Basic values of the loads ($/m^2$).....	10
4.2.2 Loads with safety factors in ULS.....	10
4.2.3 Loads with safety factors in EQ combination (§6.4.3 [2]).....	11
4.3 Loads on the full building, with safety factors in EQ combination (§6.4.3. [2])	11
4.4 Loads on independent frames.....	12
4.4.1 Loads on Frame1 (Axis C) with safety factors in EQ combination (§6.4.3 [2])	12
4.4.2 Loads on Frame2 (Axis A) with safety factors in EQ combination (§6.4.3 [2])	12
4.4.3 Loads on Frame3 (Axis 3) with safety factors in EQ combination (§6.4.3 [2])	13
4.4.4 Loads on Frame4 (Axis 1) with safety factors in EQ combination (§6.4.3 [2])	14
4.4.5 Loads on Frame5 (Axis 2) with safety factors in EQ combination (§6.4.3 [2])	15
5 Force distribution for the pushover analysis	16
6 Modeling of independent frames	17
6.1 Pushover analysis of Frame1 and Frame2	17
6.2 Pushover analysis of Frame 3, Frame 4 and Frame 5	18
7 Modeling of the 3D structure.....	21
7.1 Taking into account diaphragm effect	21
7.2 Modal analysis	21
7.3 Static pushover analysis	23
8 Determination of the target displacement (Annex B - EN 1998)	24
8.1 Modal properties	24
8.2 Design spectrum	24
8.3 Properties of the equivalent SDOF system	26
8.4 Performance of the r.c. frame	27
8.5 Summary of problems of the original r.c. frame	28
8.5.1 Effect of the axial force.....	28
8.5.2 Possibilities benefits of FRP confinement.....	29
9 Principles of rehabilitation for the structure.....	30

9.1	Rehabilitation using LGS shear walls.....	31
9.1.1	Properties of LGS steel plates used for rehabilitation.....	31
9.1.2	Performance of the strengthened structures	32
9.2	Rehabilitation by reducing the mass	35
9.3	Rehabilitation by confining the concrete in critical areas.....	36
9.4	Rehabilitation by changing the column cross-section	37
9.5	Summary of the possible rehabilitation procedures	38
10	Performance based (PBD) interpretation of the results	40
11	Conclusion.....	43

Abbreviation and terminology

CD/Capacity Diagram - plot representing the possible supply of the structure in terms of base shear, transformed in acceleration, vs. deformation (i.e. acceleration, derived from base shear vs. deformation plot).

DD/Demand Diagram - plot representing the design seismic requirements in terms of pseudo acceleration vs. deformation (i.e. pseudo acceleration vs. deformation plot).

EP - elastic plastic

EQ - earthquake

LGS - light gauge steel

PBD - performance based design

PGA - peak ground acceleration.

PSA - pseudo spectral acceleration

SD - spectral displacement

SDOF - single degree of freedom oscillator

SLS - serviceability limit state

ULS - ultimate limit state

1 Introduction

The aim of this work is to evaluate the performance of retrofitting and upgrading techniques of an r.c. frame, using Light Gauge Steel (LGS) as retrofitting material. The reference r.c. frame has been reported in detail in [3]; all properties, dimensions and loadings are based on that source.

The use of LGS is proposed as shear walls, in this report, and the performance of the LGS shear wall system is discussed.

2 FEM model development

The FEM model of the r.c. frame was developed in SEIMOSTRUCT [5]. The software is capable of modeling linear elements by dividing the cross-section in fibers. The different fibers in the section can have different material properties (e.g. yield).

In order to calibrate the model, a cantilever column has been modeled first (Figure 1), based on each cross section characteristic reported in [3]. The column has only been subjected to a horizontal force (and self weight of the column), causing bending, a small axial force and shear at the base of the column. The model is capable of taking into account axial strengths and stresses in the fibers, but shear is not accounted in the fiber model.

The concrete material has been modeled with:

- Nonlinear cracking (CC) properties with the material characteristics as in Figure 2a.
- Compression only characteristics, as in Figure 2b. In this case the tensile properties of the concrete are neglected and the compression part is tri-linear (TR).

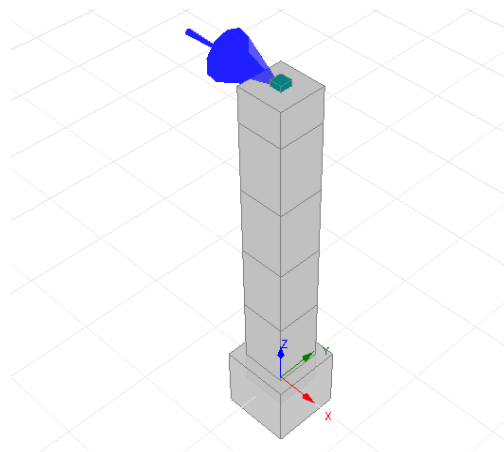


Figure 1. Column subjected to self-weight and push-over force.

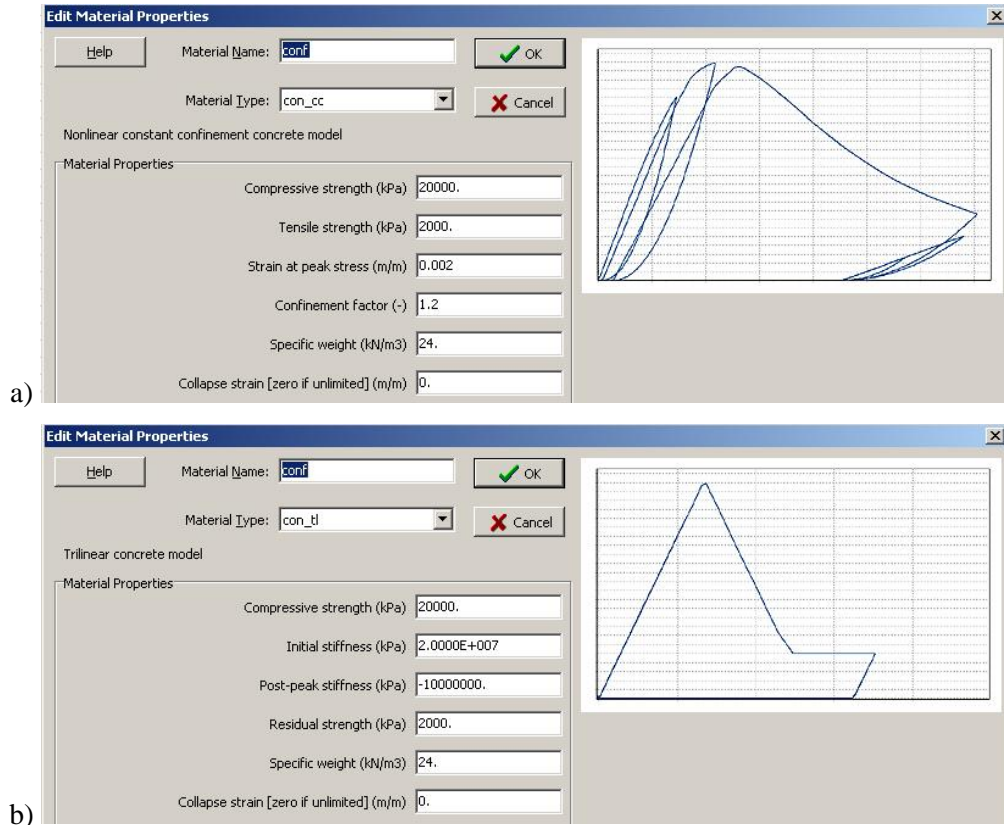


Figure 2. Nonlinear confined concrete model (a) and tri-linear concrete model (b).

The bending moment vs. displacement factor curves are presented for column cross-section (Col1 - ground floor columns) [3], using the two modeling techniques for the concrete (Figure 3). As it can be observed, the cracking modeling is predicting a more complex behavior in the tension cracking phase of the deformation, but the response is stabilized and both the moment capacity and the yield deformation are identical in the two cases.

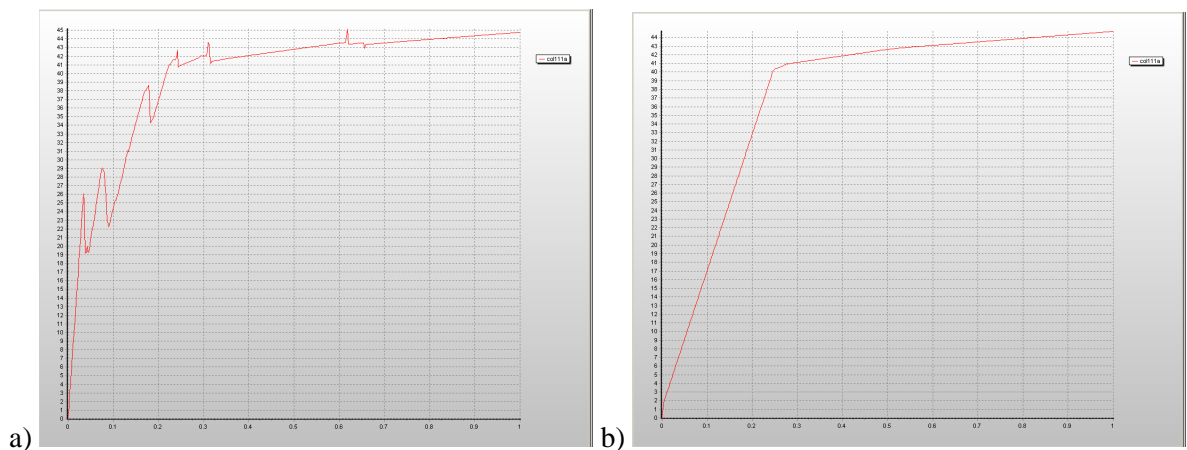


Figure 3. Force vs. displacement factor curve for Col1 using concrete modeling techniques from Figure 2.

Due to the convergence problems exhibited by the tension cracking model in case of complex models it was decided that tension cracking will be disregarded. Otherwise, both concrete constitutive models can be used in the modeling.

3 Material models

3.1 Nominal material properties

Nominal material properties have been used for the concrete and the reinforcement in all modeling, as these represent the most “likely” properties of the material of the structure. In pushover analysis, the distinction between performance with nominal properties and performance with design properties should be taken into account at the assessment of the performance of the structure.

Steel is modeled as bilinear material with the parameters. The yield strength was $f_y = 230$ MPa ($E_s = 200\,000$ MPa), and a small value of the strain hardening (1%) was accepted. The possibility of reinforcement fracture was not included in the model, but the strain level of $\delta_{s_F} = 0.04$ was monitored as ultimate strain for the reinforcing steel.

Concrete materials are modeled by a tri-linear material model. The characteristic value of the compressive strength was taken $R_{ck} = 20$ MPa ($E_C = 29\,000$ MPa). The confined concrete (i.e. inside of the reinforcement cage) retains more significant compression strength, after crushing, than the unconfined concrete outside the reinforcement cage. For the confined concrete (i.e. inside the reinforcing cage) the nonlinear concrete model was used, while for the unconfined concrete the tri-linear model. The non-linear concrete model was preferred as it is numerically more stable (i.e. because it does not contain sharp changes of stiffness), but for the spalling concrete cover it was necessary to use the tri-linear model in order to capture the very fast decrease of capacity after the reaching of the spalling strain.

The remaining compressive strength was set to: $R_{conf} = 6$ MPa & $R_{un-conf} = 2$ MPa.

- Confined concrete: $R_{ck} = 20$ MPa, strain at peak stress $\varepsilon_{peak} = 0.002$ (Figure 4)
- Unconfined concrete: $R_{ck} = 20$ MPa, $R_{un-conf} = 2$ MPa, strain at peak stress $\varepsilon_{u_N} = 0.002$, strain at complete loss of capacity $\varepsilon_0 = 0.004$ (Figure 4).

For the crushing strain of concrete the values of 0.006 (confined) and 0.002 (unconfined) are recommended [5]. However, as the structure is known to be made of very poor quality concrete, these values have been reduced. More relevant values can be determined experimentally.

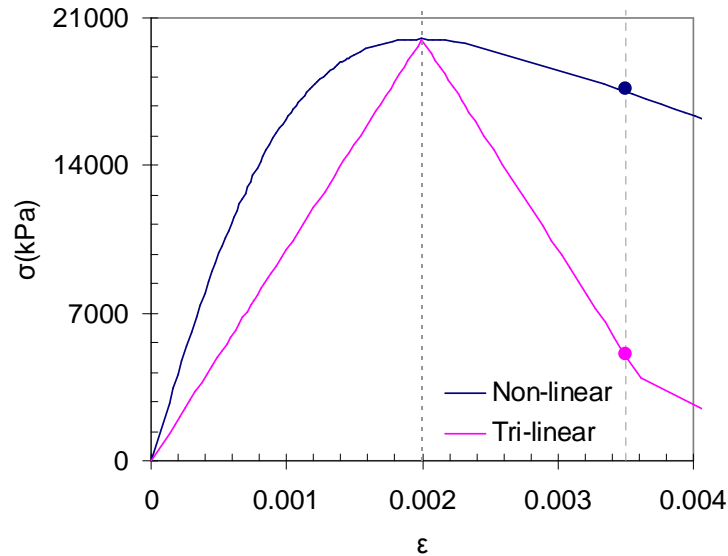


Figure 4. (a) Confined (i.e. inside the reinforcing cage) and (b) un-confined (i.e. outside of reinforcing cage) concrete material properties.

Using the safety factors: $\gamma_C = 1.5$, $\gamma_S = 1.15$, for concrete and steel strength respectively, the design values of the materials can be calculated. These are:

$$f_{y,Rd} = f_y/\gamma_S = 230/1.15 \text{ MPa} = 200 \text{ MPa} = 200 \text{ N/mm}^2$$

$$R_{ck,Rd} = R_{ck}/\gamma_C = 20/1.5 \text{ MPa} = 13.3 \text{ MPa} = 13.3 \text{ N/mm}^2.$$

These values are not used in the modeling.

3.2 Modeling of cross-sections

Cross-sections of the model are divided into 200 fibers. The fibers have one of the properties of concrete or steel base material. The division is done automatically by SEISMISOFT based on the geometry of the cross-section and the place of the reinforcing bars. Each fiber is behaving as “confined concrete”, “unconfined concrete” or “steel”.

3.3 Performance criteria

Performance criteria is monitored in the response via the material strains:

- *Cracking of the concrete* can not be detected in the models because the tensile strength of the concrete fibers is 0, so cracking is instantaneous in a concrete fiber;
- Spalling of the cover concrete is considered at ($\epsilon_{sp} = -0.002$). Fast degradation of the cover concrete capacity starts here;
- Crushing of the concrete core ($\epsilon_{crush} = -0.0035$). The concrete cover loses 75% of it’s capacity at the strain $\epsilon = -0.0035$, but the concrete core still retains 88% (Figure 4).
- Yielding of the steel reinforcement ($\epsilon_{s_N} = f_y/E_s = 0.00115$);
- Fracture of the steel reinforcement ($\epsilon_{s_F} = 0.04$).

The fracture strain of the steel reinforcement has been taken somehow randomly. Typical value recommended in [5] is 0.06. The value was reduced to 0.04 because the steel might not possess as much ductility as current grades.

It has been decided that the performance criteria will be monitored only based on material strains and not based on section curvature or chord rotation values. This later method would be less natural in case of the employed fiber-based modeling.

4 Loads on the structure

4.1 Loads other than the frame elements (/m²)

Weight of floor joists: $62.4 + 32.4 = 94.8 \text{ kg}/0.31 \text{ m}^2 = 305.8 \text{ kg/m}^2$ (daN/m²) $\approx 3 \text{ kN/m}^2$
 Concrete:

$$0.07 \times 0.2 \times 1 + 0.05 \times 0.24 = 0.026 \times 2400 = 62.4 \text{ kg/m}$$

Hollow tiles: $0.24 \times 0.15 \times 1 = 0.036 \times 900 = 32.4 \text{ kg/m}$

Weight of floor finishing: equivalent of 4cm of concrete = $96 \text{ kg/m}^2 \approx 1 \text{ kN/m}^2$

No details of the joists: 200 kg/m^2 2 kN/m^2

Finishing: 100 kg/m^2 1 kN/m^2

4.2 Total loads/floor level other than the frame elements

4.2.1 Basic values of the loads (/m²)

o Self-weights:

- Floor joists, 1st & 2nd floor: 300 daN/m^2
- Floor finishing, 1st, 2nd floors: 100 daN/m^2
- Partition walls, 1st, 2nd floor: 80 daN/m^2

§ Total 1st & 2nd floor: $300 + 100 + 80 = 480 \text{ daN/m}^2$

- Floor joist 3rd floor: 200 daN/m^2
- Floor finishing 3rd floor: 100 daN/m^2

§ Total 3rd floor: $200 + 100 = 300 \text{ daN/m}^2$

- Roof joists: 200 daN/m^2

§ Total roof: $200 = 200 \text{ daN/m}^2$

- All external walls: 250 daN/m^2 (calculated for area of the walls)

§ Total external walls: $250 = 250 \text{ daN/m}^2$

o Imposed load (not specified):

§ Occupants, 1st, 2nd floor. Category C1, Table 6.1[1]: 300 daN/m^2

§ Attic (closed to access 3rd floor). Category H, Table 6.1[1]: 40 daN/m^2

§ Roof. Category H, Table 6.6[1]: 40 daN/m^2

o Snow loads do not combine with earthquake!

4.2.2 Loads with safety factors in ULS

o Self-weight ($\gamma_{G1} = 1.35$):

- § 1st, 2nd floor distributed: $1.35 \times 480 =$ 648 daN/m²
- § 3rd floor distributed: $1.35 \times 300 =$ 405 daN/m²
- § Roof distributed: $1.35 \times 200 =$ 270 daN/m²

- § External wall distributed: $1.35 \times 250 =$ 337.5 daN/m²

- Imposed load ($\gamma_{G1} = 1.5$):
 - § 1st, 2nd floor distributed: $1.5 \times 300 =$ 450 daN/m²
 - § 3rd floor distributed: $1.5 \times 40 =$ 60 daN/m²
 - § Roof distributed: $1.5 \times 40 =$ 60 daN/m²
- Snow load:
 - § Does not combine with earthquake.

4.2.3 Loads with safety factors in EQ combination (§6.4.3 [2])

- Self-weight ($\gamma_{G1} = 1$):
 - § 1st, 2nd floor distributed: 480 daN/m²
 - § 3rd floor distributed: 300 daN/m²
 - § Roof distributed: 200 daN/m²

Imposed load are calculated taking into account the correlated occupancy of the floors ($\varphi = 0.8$ is from Table 4.2 [4], for correlated occupancy), with: $\varphi \times \psi_{21} = 0.8 \times 0.6 = 0.48$. (Obs: §4.2.4 and §3.2.4 of [4] is in contradiction of Table A1.3 of [2], so this choice is disputable.)

- Imposed load ($\varphi \times \psi_{21} = 0.48$ according to Table A1.1 in [2]):
 - § 1st, 2nd floor distributed: $0.48 \times 300 =$ 144 daN/m²
 - § 3rd floor distributed: $0.48 \times 40 =$ 19 daN/m²
 - § Roof distributed: $0.48 \times 40 =$ 19 daN/m²
- Snow load ($\psi_{21} = 0$):
 - § 0

4.3 Loads on the full building, with safety factors in EQ combination (§6.4.3. [2])

- Self-weight ($\gamma_{G1} = 1$):
 - § 1st, 2nd floor distributed: $480 \text{ daN/m}^2 \times (23 \text{ m} \times 18 \text{ m}) =$ 198720 daN
 - § 3rd floor distributed: $300 \text{ daN/m}^2 \times (23 \text{ m} \times 18 \text{ m}) =$ 124200 daN
 - § Roof distributed: $200 \text{ daN/m}^2 \times (23 \text{ m} \times 18 \text{ m}) =$ 82800 daN

- External walls ($\gamma_{G1} = 1$):
 - § 1st floor total: $250 \text{ daN/m}^2 \times (82 \text{ m} \times 3.65 \text{ m}) =$ 74825 daN
 - § 2nd floor total: $250 \text{ daN/m}^2 \times (82 \text{ m} \times 3.38 \text{ m}) =$ 69290 daN
 - § 3rd floor total: $250 \text{ daN/m}^2 \times (155.56 \text{ m}^2) =$ 38890 daN
 - § Roof total: $250 \text{ daN/m}^2 \times (14.16 \text{ m}^2) =$ 3540 daN

- Imposed load ($\varphi \times \psi_{21} = 0.48$ according to Table A1.1 in [2]):
 - § 1st, 2nd floor distributed: $144 \text{ daN/m}^2 \times (23 \text{ m} \times 18 \text{ m}) =$ 59616 daN
 - § 3rd floor distributed: $19 \text{ daN/m}^2 \times (23 \text{ m} \times 18 \text{ m}) =$ 7949 daN
 - § Roof distributed: $19 \text{ daN/m}^2 \times (23 \text{ m} \times 18 \text{ m}) =$ 7949 daN
- Snow load ($\psi_{21} = 0$):

§ 0

○ Seismic mass/floor:	
§ 1 st	333161 daN
§ 2 nd	327626 daN
§ 3 rd	171039 daN
§ Roof	94289 daN
TOTAL:	926115 daN

4.4 Loads on independent frames

4.4.1 Loads on Frame1 (Axis C) with safety factors in EQ combination (§6.4.3 [2])

○ Self-weight ($\gamma_{G1} = 1$):	
§ 1 st , 2 nd floor distributed: 4.5 m x 480 daN/m ²	2160 daN/m
§ 3 rd floor distributed: 4.5 m x 300 daN/m ²	1350 daN/m
§ Roof distributed: 4.5mx200daN/m ²	900 daN/m
○ External walls ($\gamma_{G1} = 1$):	
§ 1 st floor total: 2 x (4.5 m x 3.65 m x 250 daN/m ²)	2 x 4106 daN
§ 2 nd floor total: 2 x (4.5 m x 3.38 m x 250 daN/m ²)	2 x 3803 daN
§ 3 rd floor total: 2 x (11.1 m ² x 250 daN/m ²)	2 x 2770 daN
§ Roof total: 2 x (3.54 m ² x 250 daN/m ²)	2 x 885 daN
○ Imposed load ($\psi_{21} = 0.6$ according to Table A1.1 in [2]):	
§ 1 st , 2 nd floor distributed: 4.5 m x 144 daN/m ²	648 daN/m
§ 3 rd floor & Roof distributed: 4.5 m x 19 daN/m ²	86 daN/m
○ Total vertical loads on Frame1 (except elements of the frame):	
§ 1 st , 2 nd floor total: 2160 + 648 =	2808 daN/m
§ 3 rd floor distributed: 1350 + 86 =	1436 daN/m
§ Roof distributed: 900 + 86 =	986 daN/m
○ Seismic mass/floor in Frame1:	
§ 1 st floor: 2808 daN/m x 23 m + 2 x 4106 =	72797 daN
§ 2 nd floor: 2808 daN/m x 23 m + 2 x 3803 =	72189 daN
§ 3 rd floor: 1436 daN/m x 23m + 2 x 2770 =	38577 daN
§ Roof: 986 daN/m x 23 m + 2 x 885 =	24457 daN
TOTAL:	208020 daN

4.4.2 Loads on Frame2 (Axis A) with safety factors in EQ combination (§6.4.3 [2])

○ Self-weight ($\gamma_{G1} = 1$):	
§ 1 st , 2 nd floor distributed: 2.25 m x 480 daN/m ²	1080 daN/m
§ 3 rd floor distributed: 2.25 m x 300 daN/m ²	675 daN/m
§ Roof distributed: 2.25 m x 200 daN/m ²	450 daN/m
○ External walls ($\gamma_{G1} = 1$):	
§ 1 st floor total: 2 x (13.75 m x 3.65 m x 250 daN/m ²)	2 x 12547 daN
§ 2 nd floor total: 2 x (13.75 m x 3.38 m x 250 daN/m ²)	2 x 11619d aN
§ 3 rd floor total: 2 x ((8.46 + 9 x 1.68) m ² x 250 daN/m ²)	2 x 5895 daN

§ Roof total: $2 \times (0 \text{ m}^2 \times 250 \text{ daN/m}^2)$	0
○ Imposed load ($\varphi \times \psi_{21} = 0.48$ according to Table A1.1 in [2]):	
§ 1 st , 2 nd floor distributed: $2.25 \text{ m} \times 144 \text{ daN/m}^2$	324 daN/m
§ 3 rd floor & Roof distributed: $2.25 \text{ m} \times 19 \text{ daN/m}^2$	43 daN/m
○ Total vertical loads on Frame1 (except elements of the frame):	
§ 1 st , 2 nd floor total: $1080 + 324 =$	1404 daN/m
§ 3 rd floor distributed: $675 + 43 =$	718 daN/m
§ Roof distributed: $450 + 43 =$	493 daN/m
○ Seismic mass/floor in Frame2:	
§ 1 st floor: $1404 \text{ daN/m} \times 23 \text{ m} + 2 \times 12547 =$	57386 daN
§ 2 nd floor: $1404 \text{ daN/m} \times 23 \text{ m} + 2 \times 11619 =$	55530 daN
§ 3 rd floor: $718 \text{ daN/m} \times 23 \text{ m} + 2 \times 5895 =$	28309 daN
§ Roof: $493 \text{ daN/m} \times 23 \text{ m} =$	11344 daN
TOTAL:	152567 daN

4.4.3 Loads on Frame3 (Axis 3) with safety factors in EQ combination (§6.4.3 [2])

○ Self-weight ($\gamma_{G1} = 1$):	
§ 1 st , 2 nd floor middle concentrated: $4.5 \text{ m} \times 2.5 \text{ m} \times 480 \text{ daN/m}^2$	5400 daN
§ 1 st , 2 nd floor corner concentrated: $2.25 \text{ m} \times 2.5 \text{ m} \times 480 \text{ daN/m}^2$	2700 daN
§ 1 st , 2 nd floor distributed: $1.5 \text{ m} \times 480 \text{ daN/m}^2$	720 daN/m
§ 3 rd floor middle concentrated: $4.5 \text{ m} \times 2.5 \text{ m} \times 300 \text{ daN/m}^2$	3375 daN
§ 3 rd floor corner concentrated: $2.25 \text{ m} \times 2.5 \text{ m} \times 300 \text{ daN/m}^2$	1688 daN
§ 3 rd floor distributed: $1.5 \text{ m} \times 300 \text{ daN/m}^2$	450 daN/m
§ Roof middle concentrated: $4.5 \text{ m} \times 4 \text{ m} \times 200 \text{ daN/m}^2$	3600 daN
§ Roof corner concentrated: $2.25 \text{ m} \times 4 \text{ m} \times 200 \text{ daN/m}^2$	1800 daN
○ External walls ($\gamma_{G1} = 1$):	
§ 1 st floor total: $2 \times (4 \text{ m} \times 3.65 \text{ m} \times 250 \text{ daN/m}^2)$	2 x 3650 daN
§ 2 nd floor total: $2 \times (4 \text{ m} \times 3.38 \text{ m} \times 250 \text{ daN/m}^2)$	2 x 3380 daN
§ 3 rd floor total: $2 \times (4 \text{ m} \times 1.68 \text{ m} \times 250 \text{ daN/m}^2)$	2 x 1680 daN
○ Imposed load ($\varphi \times \psi_{21} = 0.48$ according to Table A1.1 in [2]):	
§ 1 st , 2 nd floor middle concentrated: $4.5 \text{ m} \times 2.5 \text{ m} \times 144 \text{ daN/m}^2$	1620 daN
§ 1 st , 2 nd floor corner concentrated: $2.25 \text{ m} \times 2.5 \text{ m} \times 144 \text{ daN/m}^2$	810 daN
§ 1 st , 2 nd floor distributed: $1.5 \text{ m} \times 144 \text{ daN/m}^2$	216 daN/m
§ 3 rd floor middle concentrated: $4.5 \text{ m} \times 2.5 \text{ m} \times 19 \text{ daN/m}^2$	216 daN
§ 3 rd floor corner concentrated: $2.25 \text{ m} \times 2.5 \text{ m} \times 19 \text{ daN/m}^2$	108 daN
§ 3 rd floor distributed: $1.5 \text{ m} \times 19 \text{ daN/m}^2$	29 daN/m
§ Roof middle concentrated: $4.5 \text{ m} \times 2.5 \text{ m} \times 19 \text{ daN/m}^2$	346 daN
§ Roof corner concentrated: $2.25 \text{ m} \times 2.5 \text{ m} \times 19 \text{ daN/m}^2$	173 daN
§ Roof distributed: $1.5 \text{ m} \times 19 \text{ daN/m}^2$	29 daN/m
○ Total vertical loads on Frame3 (except elements of the frame):	
§ 1 st , 2 nd floor middle: $5400 + 1620 =$	7020 daN

§ 1 st floor corner: $2700 + 810 + 3650 =$	7160 daN
§ 1 st , 2 nd floor distributed	936 daN/m
§ 2 nd floor corner: $2700 + 810 + 3380 =$	6890 daN
§ 3 rd floor middle: $3375 + 216 =$	3591 daN
§ 3 rd floor corner: $1688 + 108 + 1680 =$	3476 daN
§ 3 rd floor distributed	479 daN/m
§ Roof middle: $3600 + 346$	3946 daN
§ Roof corner: $1800 + 173$	1973 daN
○ Seismic mass/floor in Frame6:	
§ 1 st floor: $3 \times 7020 + 2 \times 7160 + 18 \times 936 =$	52228 daN
§ 2 nd floor: $3 \times 7160 + 2 \times 6890 + 18 \times 936 =$	51688 daN
§ 3 rd floor: $3 \times 3591 + 2 \times 3476 + 18 \times 479 =$	26342 daN
§ Roof: $3 \times 3946 + 2 \times 1973 =$	15782 daN
TOTAL:	146041 daN

4.4.4 Loads on Frame4 (Axis 1) with safety factors in EQ combination (§6.4.3 [2])

○ Self-weight ($\gamma_{G1} = 1$):	
§ 1 st , 2 nd floor middle concentrated: $4.5 \text{ m} \times 2.5 \text{ m} \times 480 \text{ daN/m}^2$	5400 daN
§ 1 st , 2 nd floor corner concentrated: $2.25 \text{ m} \times 2.5 \text{ m} \times 480 \text{ daN/m}^2$	2700 daN
§ 3 rd floor middle concentrated: $4.5 \text{ m} \times 2.5 \text{ m} \times 300 \text{ daN/m}^2$	3375 daN
§ 3 rd floor corner concentrated: $2.25 \text{ m} \times 2.5 \text{ m} \times 300 \text{ daN/m}^2$	1688 daN
§ Roof middle concentrated: $4.5 \text{ m} \times 2.5 \text{ m} \times 200 \text{ daN/m}^2$	2250 daN
§ Roof corner concentrated: $2.25 \text{ m} \times 2.5 \text{ m} \times 200 \text{ daN/m}^2$	1125 daN
○ External walls ($\gamma_{G1} = 1$):	
§ 1 st floor:	
• corner: $2 \times (4.75 \text{ m} \times 3.65 \text{ m} \times 250 \text{ daN/m}^2)$	2 x 4334 daN
• middle nodes: $3 \times (4.5 \text{ m} \times 3.65 \text{ m} \times 250 \text{ daN/m}^2)$	3 x 4106 daN
§ 2 nd floor:	
• corner: $2 \times (4.75 \text{ m} \times 3.38 \text{ m} \times 250 \text{ daN/m}^2)$	2 x 4014 daN
• middle nodes: $3 \times (4.5 \text{ m} \times 3.38 \text{ m} \times 250 \text{ daN/m}^2)$	3 x 3803 daN
§ 3 rd floor:	
• corner: $2 \times (8.46 \text{ m}^2 \times 250 \text{ daN/m}^2)$	2 x 2115 daN
• 2 nd node: $2 \times (9.81 \text{ m}^2 \times 250 \text{ daN/m}^2)$	2 x 2453 daN
• middle nodes: $11.1 \text{ m}^2 \times 250 \text{ daN/m}^2$	2770 daN
§ Roof:	
• corner:	0 daN
• 2 nd node: $2 \times (1.77 \text{ m}^2 \times 250 \text{ daN/m}^2)$	2 x 443 daN
• middle nodes: $3.54 \text{ m}^2 \times 250 \text{ daN/m}^2$	885 daN
○ Imposed load ($\varphi \times \psi_{21} = 0.48$ according to Table A1.1 in [2]):	
§ 1 st , 2 nd floor middle: $4.5 \text{ m} \times 2.5 \text{ m} \times 144 \text{ daN/m}^2$	1620 daN
§ 1 st , 2 nd floor corner: $2.25 \text{ m} \times 2.5 \text{ m} \times 144 \text{ daN/m}^2$	810 daN
§ 3 rd floor & Roof middle: $4.5 \text{ m} \times 2.5 \text{ m} \times 19 \text{ daN/m}^2$	216 daN
§ 3 rd floor & Roof corner: $2.25 \text{ m} \times 2.5 \text{ m} \times 19 \text{ daN/m}^2$	108 daN

○ Seismic mass/floor in Frame4:	
§ 1 st floor:	49068 daN
§ 2 nd floor:	47515 daN
§ 3 rd floor:	26269 daN
§ Roof:	11634 daN
TOTAL:	134486 daN

4.4.5 Loads on Frame5 (Axis 2) with safety factors in EQ combination (§6.4.3 [2])

○ Self-weight ($\gamma_{G1} = 1$):	
§ 1 st , 2 nd floor middle concentrated: 4.5 m x 5 m x 480 daN/m ²	10800 daN
§ 1 st , 2 nd floor corner concentrated: 2.25 m x 5 m x 480 daN/m ²	5400 daN
§ 3 rd floor middle concentrated: 4.5 m x 5 m x 300 daN/m ²	6750 daN
§ 3 rd floor corner concentrated: 2.25 m x 5 m x 300 daN/m ²	3375 daN
§ Roof middle concentrated: 4.5 m x 5 m x 200 daN/m ²	4500 daN
§ Roof corner concentrated: 2.25 m x 5 m x 200 daN/m ²	2250 daN
○ External walls ($\gamma_{G1} = 1$):	
§ 1 st floor total: 2 x (5 m x 3.65 m x 250 daN/m ²)	2 x 4563 daN
§ 2 nd floor total: 2 x (5 m x 3.38 m x 250 daN/m ²)	2 x 4225 daN
§ 3 rd floor total: 2 x (5 m x 1.68 m x 250 daN/m ²)	2 x 2100 daN
○ Imposed load ($\varphi \times \psi_{21} = 0.48$ according to Table A1.1 in [2]):	
§ 1 st , 2 nd floor middle concentrated: 4.5 m x 5 m x 144 daN/m ²	3240 daN
§ 1 st , 2 nd floor corner concentrated: 2.25 m x 5 m x 144 daN/m ²	1620 daN
§ 3 rd floor & Roof middle: 4.5 m x 5 m x 19 daN/m ²	432 daN
§ 3 rd floor & Roof corner: 2.25 m x 5 m x 19 daN/m ²	216 daN
○ Total vertical loads on Frame5 (except elements of the frame):	
§ 1 st , 2 nd floor middle: 10800 + 3240 =	14040 daN
§ 1 st floor corner: 5400 + 1620 + 4563 =	11583 daN
§ 2 nd floor corner: 5400 + 1620 + 4225 =	11245 daN
§ 3 rd floor middle: 6750 + 432 =	7182 daN
§ 3 rd floor corner: 3375 + 216 + 2100 =	5691 daN
§ Roof middle: 4500 + 432 =	4932 daN
§ Roof corner: 2250 + 216 =	2466 daN
○ Seismic mass/floor in Frame5:	
§ 1 st floor: 3 x 14040 + 2 x 11583 =	65285 daN
§ 2 nd floor: 3 x 14040 + 2 x 11245 =	64610 daN
§ 3 rd floor: 3 x 7182 + 2 x 5691 =	32928 daN
§ Roof: 3 x 4932 + 2 x 2466 =	19728 daN
TOTAL:	182551 daN

Table 1. Summary of load distribution (without self weight of the structure).

Axis	A & E	B & D	C	1 & 6	2 & 5	3 & 4	Total
Frame	X direction			Y direction			3D
	1	NA	2	4	5	3	
	(daN)	(daN)	(daN)	(daN)	(daN)	(daN)	(daN)
1 st floor	57386	72797	72797	49068	65285	52228	333161
2 nd floor	55530	72189	72189	47515	64610	51688	327626
3 rd floor	28309	37942	38577	26269	32928	26342	171079
Roof	11344	23572	24457	11634	19728	15782	94289
Total	152567	206500	208020	134486	182551	146041	926155

5 Force distribution for the pushover analysis

The simplified pushover analysis of each frame takes into account the vertical forces acting on the frame in the earthquake combination together with a steadily increasing lateral force. This lateral force distributed to the different floor levels according to the supposition of linearly increasing lateral displacements (i.e. according to §4.3.3.2.3 of [4]):

$$F_i = F_b \cdot \frac{h_i \cdot m_i}{\sum_{j=1}^n h_j \cdot m_j} \quad (1)$$

Where F_i is the force corresponding to mass i
 F_b is the total base shear corresponding to the masses acting on the frame
 h_i is the height of mass i
 m_i is mass i
 h_j is the height of mass j
 m_j is mass j
 n is the number of concentrated masses.

At this stage it is important to determine the distribution of the lateral forces corresponding to the pushover analysis (and not their values). For Frame 1 and Frame 2 the distribution of the horizontal forces is also almost identical, with slight differences due to the presence of the external wall on Frame 2 (Table 2). The situation is similar for Frame 3, Frame 4 and Frame 5, where the distribution of the horizontal loads almost identical (Table 2).

Table 2. Distribution of the horizontal loads in each frame and the 3D structure.

	Level	h(m)	$m_{total-i}(t)$	Φ_j	$m \times \Phi_j$	F(%) / Level	Nodes / Level	F / Node
Frame 1	1	3.9	96.8	0.31	30.3	18.1	6	3.0223
	2	7.3	94.3	0.59	55.3	33.1	6	5.5088
	3	10.65	52.9	0.86	45.3	27.1	6	4.5141
	R1	12.45	36.3	1	36.3	21.7	6	3.6215
	Sum:		280.3		167.2	100.0		
Frame 2	1	3.9	81.7	0.37	29.9	21.7	6	3.6116
	2	7.3	77.9	0.69	53.4	38.7	6	6.4447
	3	10.65	54.8	1	54.8	39.7	6	6.6103
	Sum:		214.4		138.1	100.0		

	Level	h(m)	$m_{total-i}(t)$	Φ_j	$m \times \Phi_j$	F(%) / Level	Nodes / Level	F / Node
Frame 3	1	3.9	66.8	0.31	20.9	19.3	5	3.8515
	2	7.3	65.2	0.59	38.3	35.2	5	7.0395
	3	10.65	40.3	0.86	34.5	31.8	5	6.3515
	R1	11.55	10.3	0.93	9.5	8.8	2	4.3938
	R2	12.45	5.4	1	5.4	5.0	1	4.9997
		Sum:		188.1		108.7	100.0	
Frame 4	1	3.9	62.1	0.31	19.5	19.8	5	3.955
	2	7.3	59.5	0.59	34.9	35.5	5	7.0929
	3	10.65	37.0	0.86	31.6	32.1	5	6.4298
	R1	11.55	8.2	0.93	7.6	7.7	2	3.8542
	R2	12.45	4.8	1	4.8	4.9	1	4.9032
		Sum:		171.7		98.4	100.0	
Frame 5	1	3.9	77.3	0.31	24.2	19.5	5	3.9038
	2	7.3	73.9	0.59	43.3	34.9	5	6.9815
	3	10.65	45.2	0.86	38.7	31.2	5	6.2374
	R1	11.55	12.3	0.93	11.4	9.2	2	4.5981
	R2	12.45	6.4	1	6.4	5.2	1	5.1904
		Sum:		215.1		124.0	100.0	

Note: $m_{total-i}$ is the total mass in the earthquake combination, including loads and self weight.

6 Modeling of independent frames

6.1 Pushover analysis of Frame1 and Frame2

The vertical loads from Table 1 have been applied to Frame 1, together with an increasing lateral/horizontal load corresponding to values in Table 2. The pushover curve (storey drift vs. total base shear) corresponding to each storey is presented in Figure 5(a). The deformed shape of Frame 1 is presented in Figure 6(a).

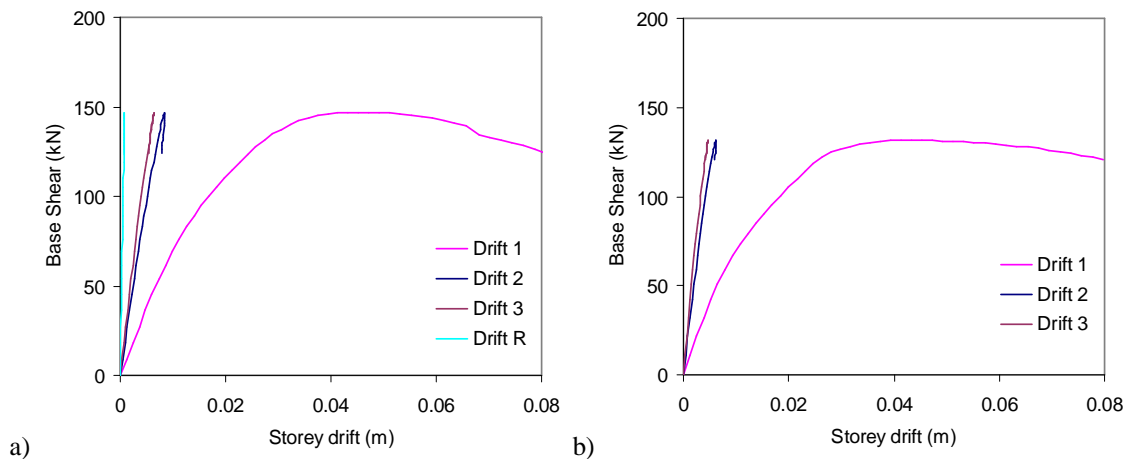


Figure 5. Storey-drift history during pushover of (a) Frame 1 and (b) Frame 2.

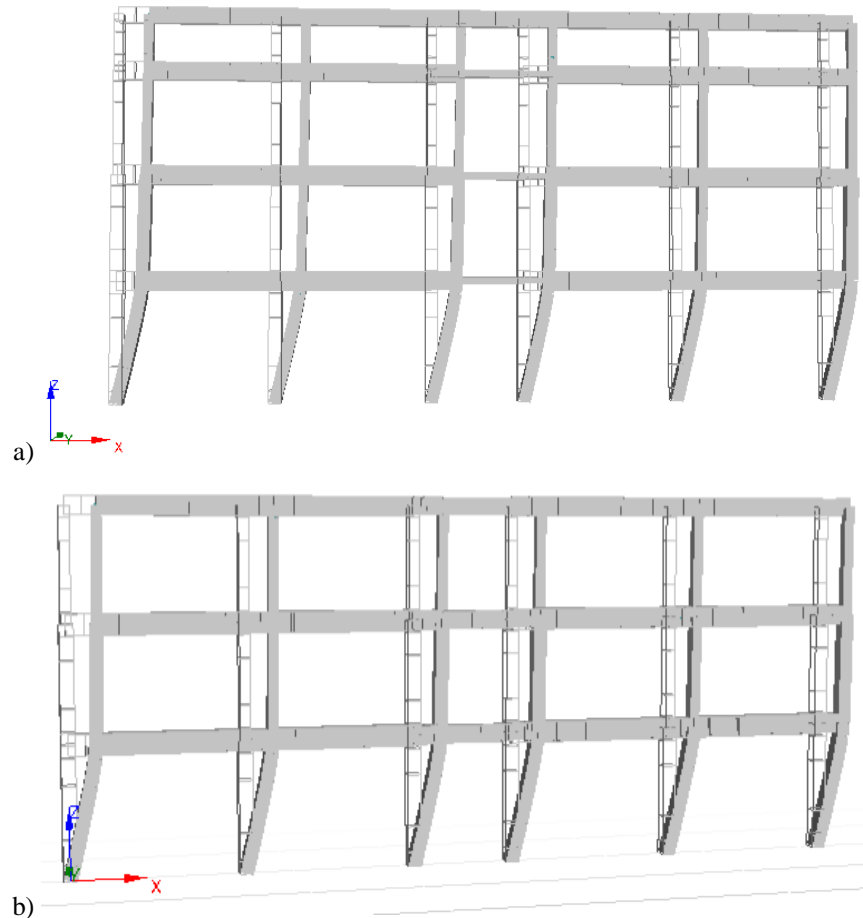


Figure 6. Deformed shape of (a) Frame 1 ($d_{3rd\,floor} = 0.094\,m$) and (b) Frame 2 ($d_{3rd\,floor} = 0.090\,m$).

It is evident from Figure 5(a) that the frame develops a storey mechanism between the ground and the first slab level (Drift 1). Beyond the displacement presented in Figure 5, the model is not convergent, because further displacement generates crushing of significant number of concrete fibers (with sudden reduction of the capacity of the frame). The crushing develops as a result of high axial forces on columns of Frame 1.

Pushover analysis was also carried out for Frame 2. Vertical loads were fixed (i.e. values from Table 1), and gradually increasing horizontal load was applied to the frame. The inter-storey drift histories are presented in Figure 5(b), and the deformed shape in Figure 6(b). From both figures it is evident that Frame 2 develops identical mechanism as Frame 1 (Drift 1). The other two levels remain essentially elastic.

The displacement at the 3rd floor level vs. the base shear force is presented in Figure 9. The effect of vertical forces is that it (i) increases the base shear force resisted by the frames, but it (ii) reduces ductility because concrete fibers are more loaded in compression.

6.2 Pushover analysis of Frame 3, Frame 4 and Frame 5

Together with the vertical loads in the earthquake combination (Table 1. Summary of load distribution (without self weight of the structure).), the

horizontal pushover is producing the drifts presented in Figure 7. As it can be seen from the curves, all frames develop a global failure mode involving all floors (i.e. except the roof level). This happens because the beams are much weaker than the columns, and the design resembles the weak beam/strong column concept recommended in modern design codes.

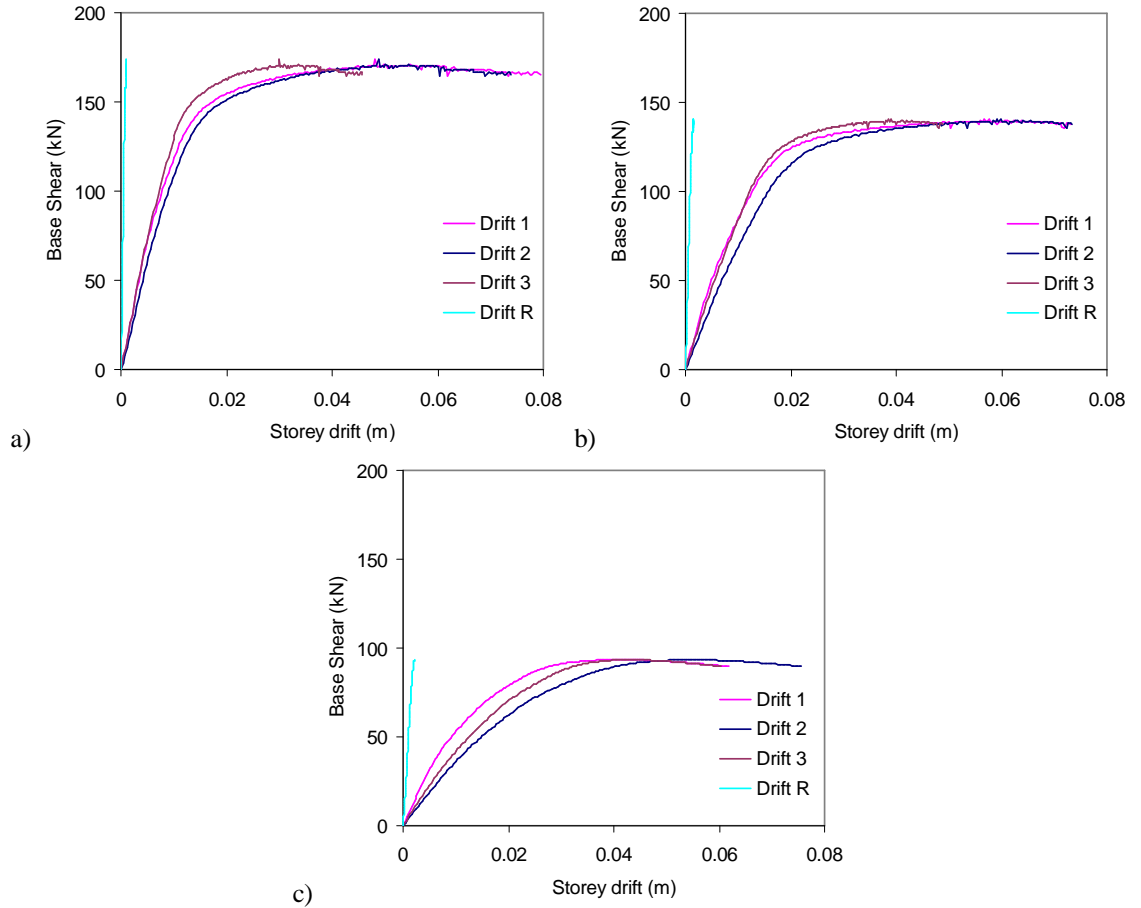


Figure 7. Storey drift curves of (a) Frame 3, (b) Frame 4 & (c) Frame 5.

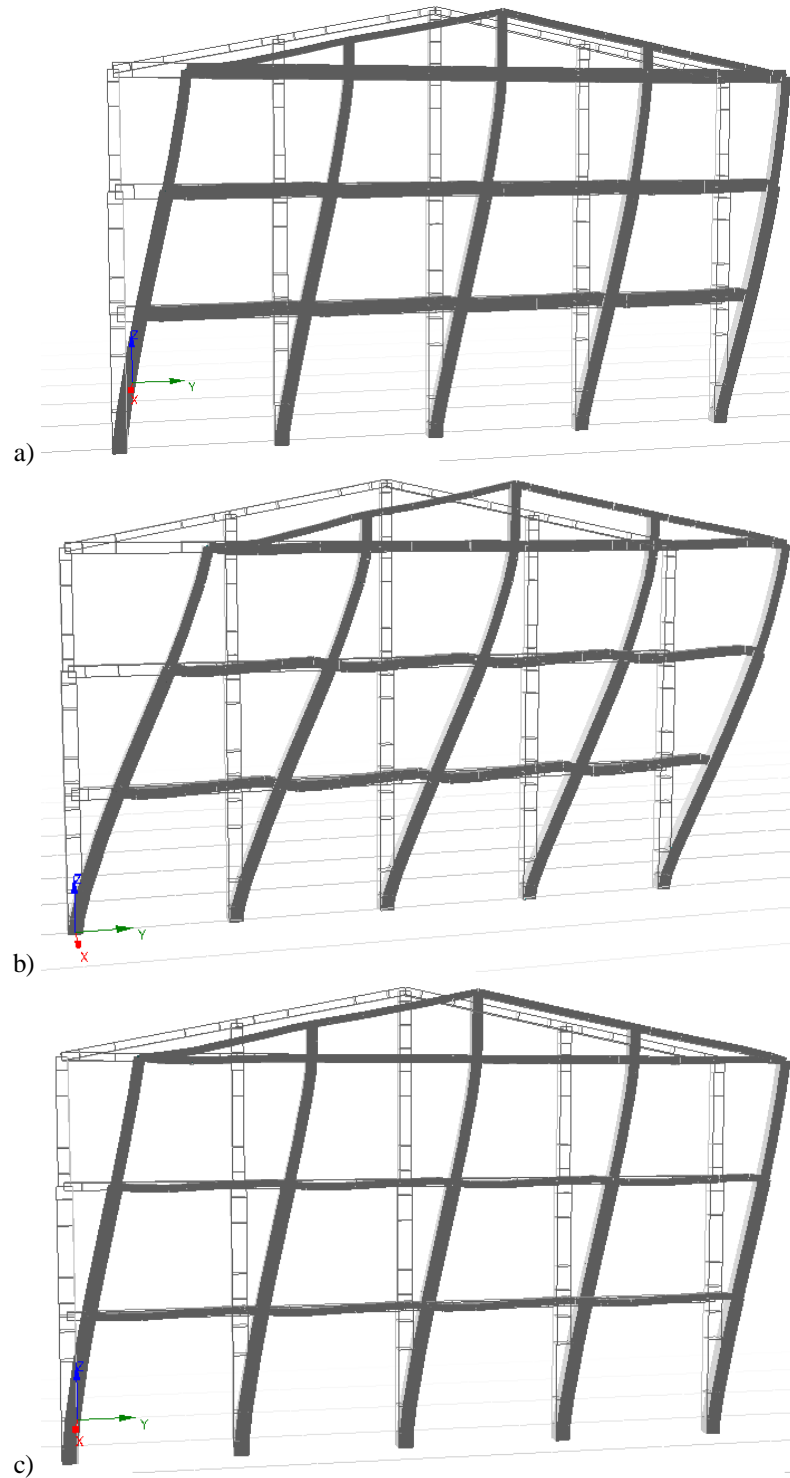


Figure 8. Deformed shapes of (a) Frame 3 (b) Frame 4 and (c) Frame 5 at $d_{roof} = 0.20 \text{ m}$

The displacement of the roof vs. the base shear for the frames is represented in Figure 9b. Like previously, 3 versions of each frame were analyzed: without vertical loads and nominal material properties (Frame 3, 4 & 5); together with vertical loads and with nominal material properties (Frame 3v, 4v & 5v) and with vertical loads but with design material properties. The rigidity and strength values for each frame are summarized in Table 3.

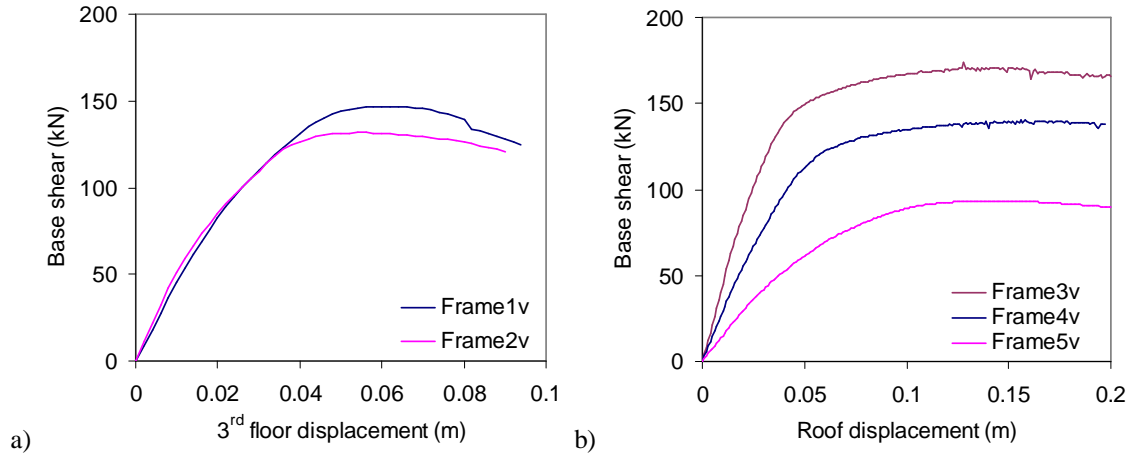


Figure 9. Pushover curves of the frames in the X (a) and Y (b) direction.

Table 3. Rigidity and strength of frames.

	Frame1v	Frame2v	Frame3v	Frame4v	Frame5v
K_{ini} (kN/m)	4464	4994	4592	2723	1410
K_{crack} (kN/m)	2732	2749	2566	1774	807
F_{max} (kN)	146.74	131.64	173.88	140.67	93.41

7 Modeling of the 3D structure

7.1 Taking into account diaphragm effect

In order to correctly distribute the horizontal loads at floor levels, it is important to take into account the diaphragm effect of the slabs in the frame. As SEISMOSTRUCT does not have the facility of the floor diaphragm implemented, the slabs were modeled as equivalent cross-braces at each floor + roof level.

According to the recommendation of the help system; for square panels the axial stiffness of each brace $(E_{br} \cdot A_{br})/L_{br}$ must be approximately equal to 35% the stiffness of the slab $K_s = \frac{1}{L^3/(12 \cdot E_{con} \cdot I_{wall}) + L/(A_{wall} \cdot G_{con})}$. Most slab cells in the

frame are 5 m × 4.5 m; while the thickness of the floor slab is of 5 cm [3]. If we assimilate these slabs as $L = 5$ m, $E_{con} = 2 \cdot 10^7$ kPa, $G_{con} = 0.416 \cdot E_{con} = 0.832 \cdot 10^7$ kPa, $A = 0.05 \cdot 5 = 0.25$ m², $I = 0.05 \cdot 5^3/12 = 0.5208$ m⁴, and use a bracing material 10 times stiffer than steel ($E_{br} = 2 \cdot 10^9$ kPa), the diameter of the “equivalent” circular cross-bracing replacing the slab results to be 1.5 cm ($A_{br} = 17.52$ cm²). The diaphragm effect of all floors and the roof was modeled using cross-bracings of this diameter.

7.2 Modal analysis

The distributed vertical loads were placed on the 3D structure according to values presented in Table 1. The structure had a total self-weight of $m_{self} = 413.7$ t (Table 5), while the total mass, including loads in the earthquake combination was $m = 1357.6$ t (Table 5).

The vibration modes of the 3D frame have been determined using both the self-weight and the vertical load (1357.6 t). The vibration modes and periods of vibration are presented in Table 4.

It can be observed that the frame is weaker in the X direction, compared to the Y direction. The fact that translational and torsional modes are very close to each other indicates that the frame might be torsionally sensitive (see. §4.3.3.4.2.7 of [4]). Torsionally sensitive structures are vulnerable to increase of the deformations compared to the estimates of a pushover analysis, and sensitivity can be reduced by placing Y-direction bracing far from the centre of mass.

Table 4. Vibration modes of the 3D model (without and with the vertical loads).

Mode	Mode type	T(s)	Self-weight + vertical loads			
			$M_x(t)$	$M_y(t)$	$M_x(\%)$	$M_y(\%)$
1	X Trans	1.09	1316	0	97	0
2	Y Trans	1.00	0	1131	0	83
3	Torsion	0.89	0	0	0	0
4	X 2 nd	0.33	24	0	2	0
5	Y 2 nd	0.32	0	154	0	11
6	Torsion 2 nd	0.30	0	0	0	0

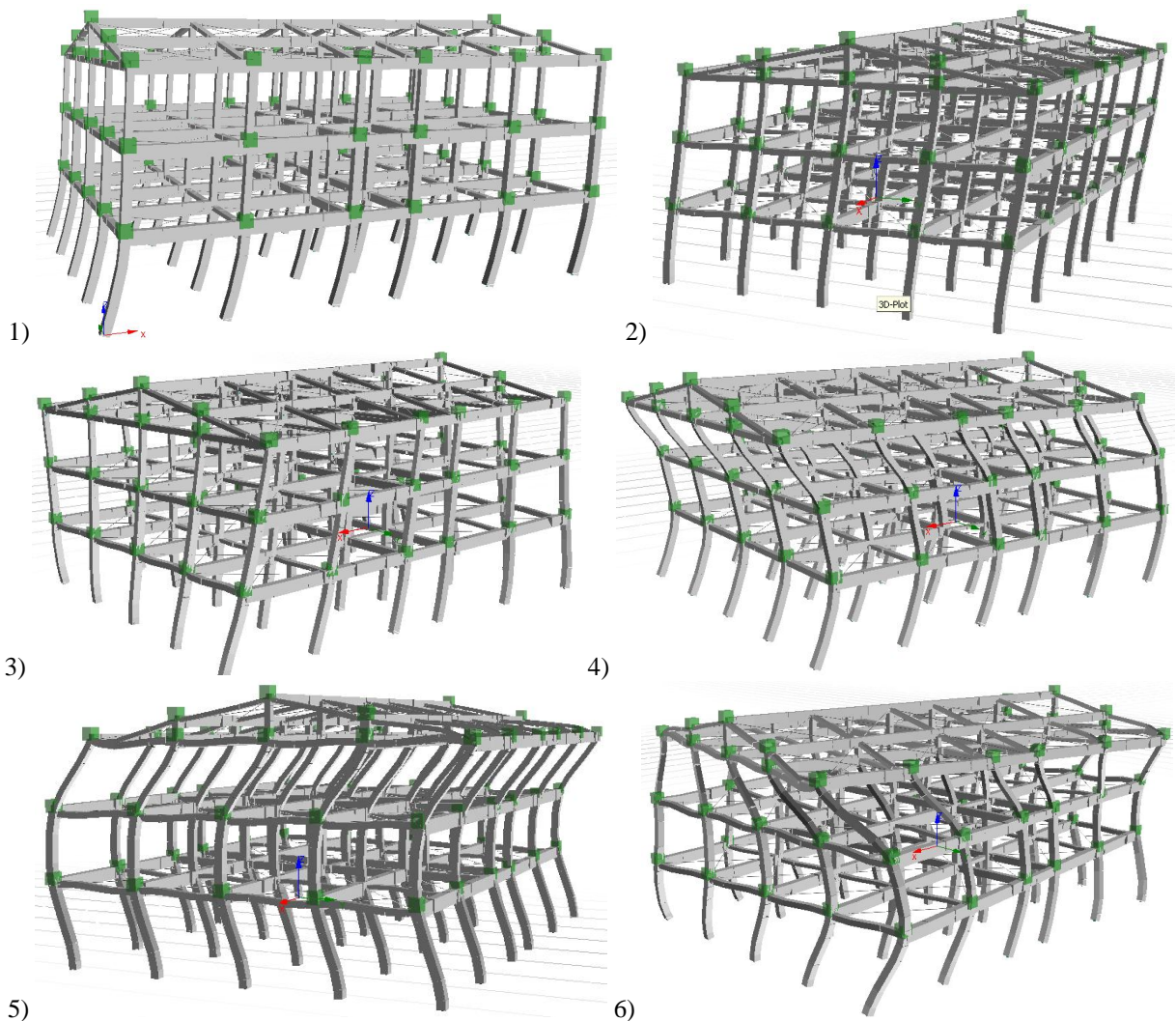


Figure 10. Vibration modes of the 3D frame (with vertical loads).

7.3 Static pushover analysis

The horizontal loads were distributed to the different levels of the frame according to Table 5.

Table 5. Distribution of the horizontal loads in the 3D structure.

	Level	h(m)	$m_{self-i}(t)$	$m_{load-i}(t)$	$m(t)$	$h_i * m_i$	$F_i(\%)/Level$	Nodes/Level	$F_i/Node$
X or Y direction	1	3.9	139.8	339.6	479.4	150.2	19.1	30	0.635
	2	7.3	130.2	333.9	464.2	272.2	34.5	30	1.151
	3	10.65	95.0	197.3	292.3	250.1	31.7	30	1.057
	Roof	11.55	31.3	48.0	79.3	73.6	9.3	12	0.778
		12.45	17.4	24.9	42.3	42.3	5.4	6	0.894
Total:			413.7	943.8	1357.6	788.3	100.0		

The static pushover curve in the X and Y direction, using the vertical loads and the horizontal loads according to Table 5 is presented in Figure 11. The deformation of the frames was equalized by the floor diaphragms considered in the analysis, and deformed shape of the 3D structure is represented from a lateral view in Figure 12.

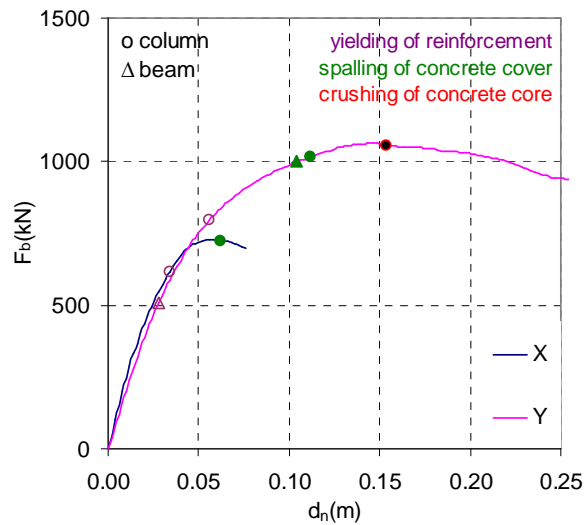


Figure 11. Static pushover curves of the 3D frame in the X and Y direction.

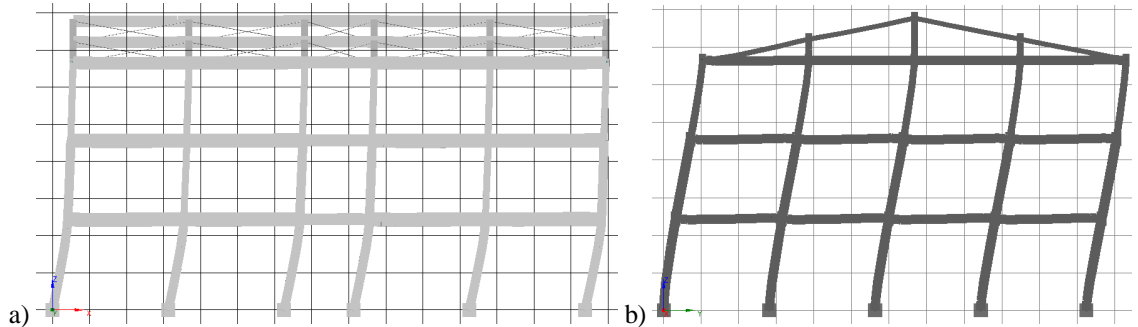


Figure 12. Deformation in the last step captured with design values of material properties: (a) X, (b) Y direction.

8 Determination of the target displacement (Annex B - EN 1998)

8.1 Modal properties

The modal properties of the frame, in the first translational mode in the X and Y directions are calculated based on Table 6. Annex B of [4] is followed in notation and methodology.

Table 6. Basic quantities for the modal properties.

Level	$m_{self-i}(t)$	$m_{load-i}(t)$	$m_i(t)$	$h_i(m)$	Φ_i	$m_i \times \Phi_i$	$m_i \times \Phi_i^2$	$h_i \times m_i \times \Phi_i$	$F_i(\%)/Level$
1	139.8	339.6	479.4	3.9	0.31	150.2	47.0	585.7	19.1
2	130.2	333.9	464.2	7.3	0.59	272.2	159.6	1986.9	34.5
3	95.0	197.3	292.3	10.65	0.86	250.1	213.9	2663.2	31.7
	31.3	48.0	79.3	11.55	0.93	73.6	68.3	850.0	9.3
	17.4	24.9	42.3	12.45	1	42.3	42.3	526.5	5.4
Sum:	413.7	943.8	1357.6			788.3	531.1	6612.4	100.0

In the first mode we have the following modal parameters [6]:

- The “modal participation factor”:

$$\Gamma_1 = \frac{\sum m_i \cdot \Phi_i}{\sum m_i \cdot (\Phi_i)^2} = 1.48$$
- The modal height:

$$h_1^* = \frac{\sum h_i \cdot m_i \cdot \Phi_i}{\sum m_i \cdot \Phi_i} = 8.39m$$
- The modal mass:

$$M_1^* = \frac{(\sum m_i \cdot \Phi_i)^2}{\sum m_i \cdot (\Phi_i)^2} = 1170.05t$$

8.2 Design spectrum

The supposed loading of the frame corresponds to Type 1 spectra, on soil type B, and with high seismicity ($a_g = 0.23 \times g$). Soil type B implies that the design spectrum is characterized by: $T_B = 0.15$ s, $T_C = 0.5$ s, $T_D = 2$ s and $S = 1.2$ (Table 3.2 [4]).

The importance class of the building is III (Table 4.3, [4]) with $\gamma_I = 1.2$. (NOTE: According to 3.2.2.1.(6) of [4] the topographic amplification should be taken into account - Annex A of EN1998-5. This was not done here.)

According to Eq. 6.12b of [2], the combination of actions for the seismic design situation is:

$$\sum_{j \neq 1} G_{k,j} + P + A_{Ed} + \sum_{i \geq 1} \Psi_{2,i} \cdot Q_{k,i} \quad (2)$$

Where: $G_{k,j}$ - is the characteristic value of the permanent action j
 P - representative value of pre-stressing
 A_{Ed} - the design value of the seismic action
 $\psi_{2,i} \times Q_{k,i}$ - quasi-permanent value of the variable action i .

According to Table A1.3 of [2], $A_{Ed} = \gamma_I \times A_{Ek}$, where A_{Ek} is the characteristic value of the seismic action. A_{Ek} is represented in [4] by the elastic response spectrum ($S_{e(T)}$) and design response spectrum ($S_{d(T)}$). In a simplified, lateral force, analysis the base shear force F_b can be calculated in any direction of the structure as (Eq. 4.5 of [4]):

$$F_b = S_{d(T_1)} \cdot m \cdot \lambda$$

Where: $S_{d(T_1)}$ - is the ordinate of the design spectrum corresponding to T_1
 m - is the total mass
 λ - is 0.85 if the building has more than 2 levels, and $T_1 < 2 \times T_C = 4$
 s

If only elastic response of the structure is expected the base shear force can be calculated as: $F_{be} = S_{e(T_1)} \cdot m \cdot \lambda$ where $S_{e(T_1)}$ is the ordinate of the elastic spectrum corresponding to T_1 . The elastic spectrum generated base shear force, corresponding to A_{Ed} in our case is:

$$F_{be} = \gamma_I \cdot (S_{e(T_1)} \cdot m \cdot \lambda) = 1.2 \cdot (S_{e(T_1)} \cdot m \cdot 0.85) = (1.02 \cdot S_{e(T_1)}) \cdot m \quad (3)$$

The elastic spectrum S_e was calculated according to §3.2.2.2 [4]. Further, the spectral displacement was calculated as $s_{ed} = \left(\frac{T}{2 \cdot \pi}\right)^2 \cdot S_e$. It can be seen that both can simply be multiplied by 1.02 in order to obtain the value corresponding to A_{Ed} . The two spectrums, $(1.02 \times S_e)$ and $(1.02 \times S_{ed})$ are presented in Figure 13. In Figure 14, S_e is represented in function of S_{ed} , forming the elastic demand diagram corresponding to A_{Ed} . This curve represents the requirements on the structure.

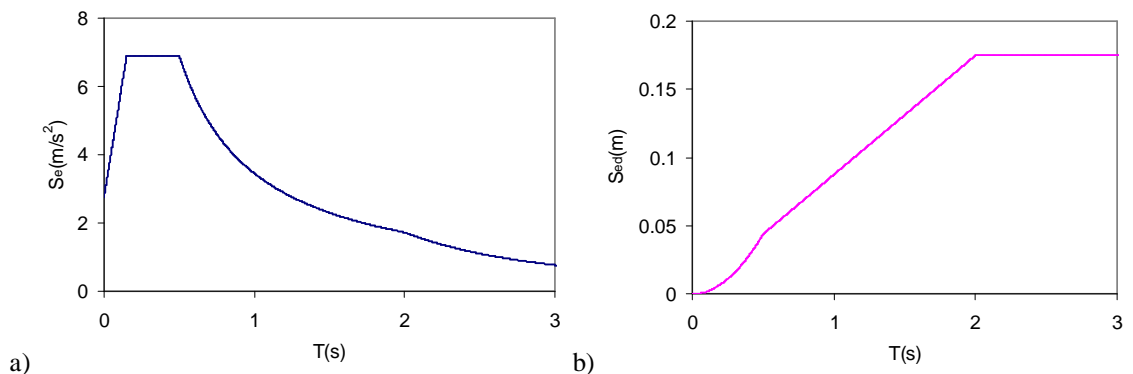


Figure 13. Pseudo-acceleration (S_e) and displacement (S_{ed}) response spectrums corresponding to A_{Ed} .

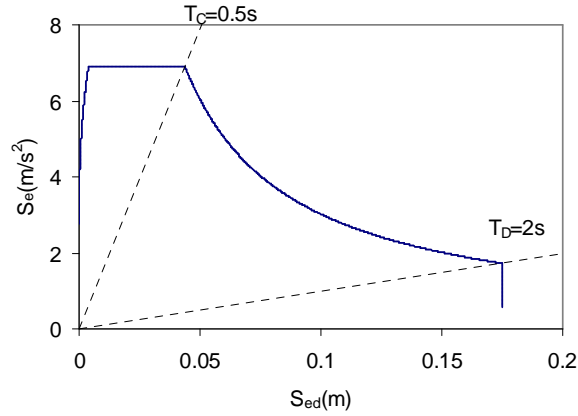


Figure 14. Demand diagram corresponding to the local seismic conditions.

8.3 Properties of the equivalent SDOF system

The pushover curves presented in Figure 11 have to be transformed in capacity diagram ($S_{ed} - S_e$) format in order to become compatible with the demand diagram from Figure 14.

The transformation is according to Annex B of EN 1998 [4] as:

$$F^* = \frac{F_b}{\Gamma_1} \quad \& \quad d^* = \frac{d_n}{\Gamma_1}; \quad S_e(T^*) = \frac{F^*}{m^*} \quad (4)$$

Where F_b is the base shear force of the MDOF system (Figure 11);
 F^* is the base shear of the equivalent SDOF system;
 d_n is the displacement of the control node ($n = 353$, top node in this case) of the MDOF system (Figure 11);
 d^* is the deformation of the equivalent SDOF system.

The values of the base shear force on the equivalent SDOF system can be further in pseudo-spectral acceleration (S_e) as:

$$S_e(T^*) = \frac{F^*}{\sum m_i \cdot \Phi_i}, \quad \text{where } \sum m_i \cdot \Phi_i = m^* \text{ is the "mass of the equivalent SDOF" (Annex B, [4]).}$$

In fact this transformation can be done directly from F_b , by:

$$S_e(T^*) = \frac{F_b}{M_1^*}, \quad \text{where } M_1^* \text{ is indeed the modal mass (mass of the equivalent SDOF) [6]}$$

In fact the two relations are equivalent because:

$$S_e(T^*) = \frac{F_b}{M_1^*} = \frac{F_b}{\frac{\sum m_i \cdot \Phi_i}{\sum m_i \cdot (\Phi_i)^2} \cdot \sum m_i \cdot \Phi_i} = \frac{F_b}{\Gamma_1 \cdot m^*} = \frac{F^*}{m^*}$$

The idealized elasto-plastic force displacement diagrams, and properties, have been determined based on the capacity diagram in F^* vs. d^* format. For this purpose the methodology presented in Annex B [4] has been used. The capacity diagrams, together with their elasto-plastic (EP) equivalents are presented in Figure 15. The curves are represented both using the mean value of the material properties and the design value.

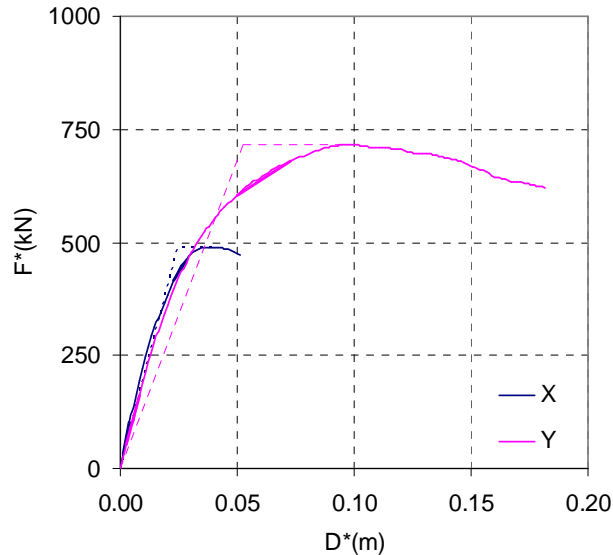


Figure 15. Equivalent elasto-plastic displacement relationship derived from the capacity curves.

8.4 Performance of the r.c. frame

The pushover curves from Figure 11 transformed in $S_e(T^*)$ vs. d^* format were superimposed on the demand diagram (Figure 14) in Figure 16.

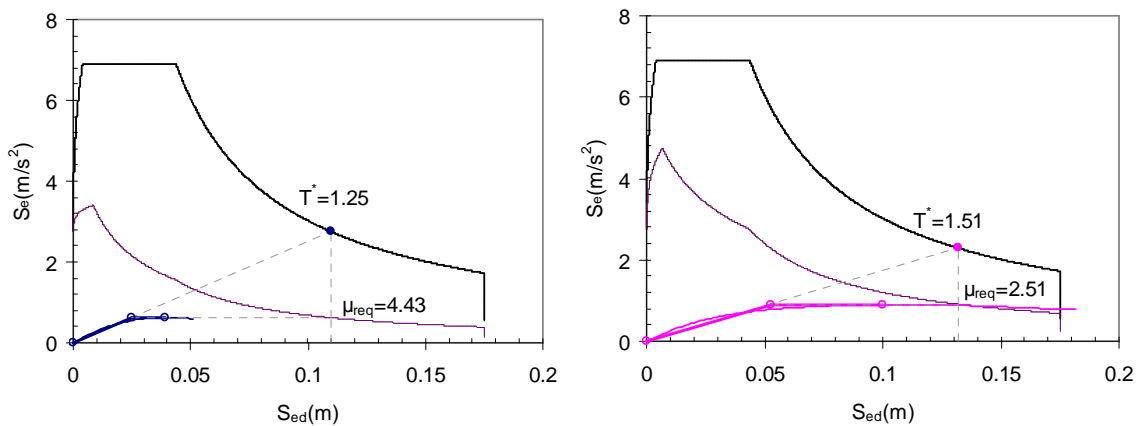


Figure 16. Demand and capacity diagrams.

It results from the capacity vs. demand diagram presented in Figure 16 that the required a q factor for the design of the frame is about $q_{\text{req-x}} = 4.5$ in the X direction, and $q_{\text{req-y}} = 2.5$ in the Y direction. This is equivalent of a ductility requirement of about $\mu_{\text{req-x}} = 4.5$, and $\mu_{\text{req-y}} = 2.5$ of the equivalent SDOF system. Such displacement requirement translates to a required top displacement of the frame of $D_x = 16$ cm and $D_y = 20$ cm.

It appears from the model that the frame can sustain a ductility level closer to $\mu_{\text{ava-x}} = 1.6$ and $\mu_{\text{ava-y}} = 1.9$. Two solutions can be adopted for the rehabilitation of the frame: (i) improving the global ductility in both directions or (ii) increasing the lateral load bearing capacity of the frame. The increasing of ductility seems plausible in the Y direction, but questionable in the X direction where the required ductility is very high.

8.5 Summary of problems of the original r.c. frame

Problems with the initial r.c. structure are:

- ... it is possible that the frame is torsion sensitive ($T_{\text{Tors}} \sim T_{\text{Xtrans}}$);
- ... it is weak in both X and Y direction;
- ... it is flexible in both directions; the values of $T_x^* = 1.25$ s and $T_y^* = 1.51$ s are quite large;
- ... results of the elastic modeling are completely misleading and they should not be used alone in any assessment;
- ... at the existing level of compression force, columns tend to fail by crushing of the concrete;
- ... in the X direction the structure is weak-column/strong-beam structure, (the opposite to the one suggested by design codes).

One of the most disturbing of these problems is the fact that axial forces in columns are very high compared to the capacity of the columns. This leads to sudden (crushing) failure of the concrete in the columns, at very low values of the lateral displacement (see Figure 11). Even if parallel load bearing systems are activated below these displacement values, the columns of the frame are still under high compression and they will fail suddenly at these displacement values.

8.5.1 Effect of the axial force

The limited available ductility in both directions of the structure is due to the effect of the axial force in the ground floor columns. As presented in Figure 17, at high axial force levels, the lateral displacement corresponding to the yielding of the tensile reinforcement (i.e. a ductile failure) and the one corresponding to crushing of the compressed concrete (i.e. a fragile failure) are coming very close to each other. At $N = 800$ kN axial force, the yielding and crushing occurs at the same lateral displacement (~ 0.019 m). At higher axial load crushing precedes yielding, resulting in fragile failure of the column.

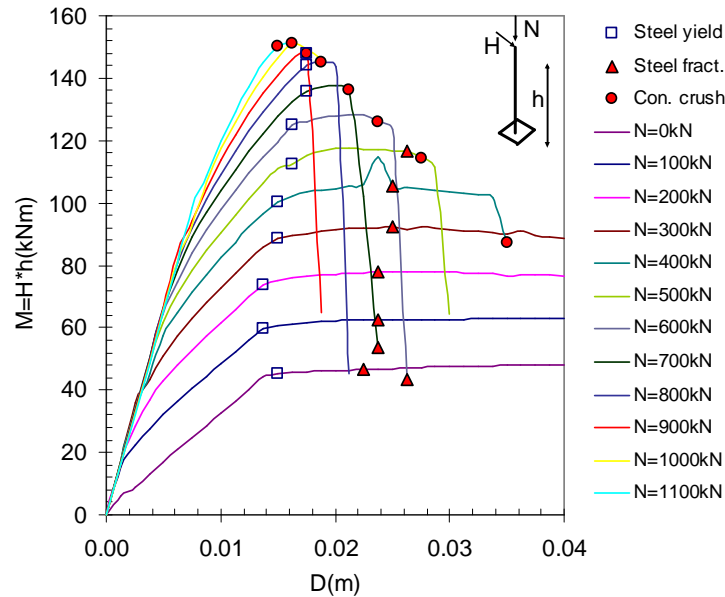


Figure 17. Effect of the axial force on the ductility of columns on the ground floor (type Col1).

In the 3D structural model columns are loaded with:

- Axial force $N \sim 600$ kN, ground floor columns B2, C2, D2, B5, C5, D5 (Col1);
- Axial force $N \sim 470$ kN, columns B3, C3, D3, B4, C4, D4 (Col1);
- Axial force $N \sim 430$ kN, columns B2, C2, D2, B6, C6, D6 (Col1);
- Axial force $N \sim 460$ kN, columns A2, D2, A5, D5 (Col1).

If this data is correlated with Figure 17, it can be seen that columns with 600 kN axial force have very little ductility, because the failure of these columns is governed by the crushing of the concrete.

8.5.2 Possibilities benefits of FRP confinement

In order to achieve a failure by yielding of the reinforcing bars, columns with the largest values of axial force can be confined at upper and lower ends by applying FRP bandaging. Let us assume that such FRP bandaging can increase the concrete strength by 80% to $R_{ck_FRP} = 36000$ kPa. This corresponds to a crushing strain of $\delta_{s_N_FRP} = -R_{ck_FRP}/E_c = -0.0018$, ($R_{confined} = 10800$ kPa).

If this improvement of the concrete quality is applied to the bottom 30% height of the column, the pushover curves presented in Figure 18 are obtained. As it can be observed, with values of the improved material properties - Mean (+80% FRP) case - the ductility is very good. The concrete does not crush, and the fracture of the steel reinforcement governs the failure mode.

Therefore, it can be concluded that any measure of providing ductility by confining the concrete in critical regions (i.e. potential plastic hinges at column ends with high compression), should aim at a substantial increase of R_{ck} .

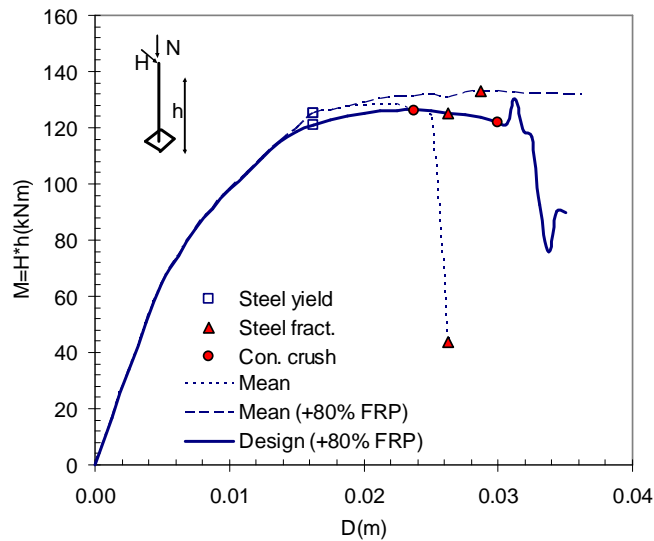


Figure 18. Pushover curves with different concrete quality ($N = 600 \text{ kN}$).

9 Principles of rehabilitation for the structure

At the reference frame, at $d_{lim} = 0.06 \text{ m}$ in the X direction, and $d_{lim} = 0.15 \text{ m}$ at Y direction (Figure 11) the concrete fibers of some columns start to crush. Therefore, any rehabilitation method not influencing the columns shape and load (e.g. shear walls, dissipaters etc.) should be made so that it does not allow larger displacement demands than these values. If the displacement demand is larger the same concrete fibers in column are crushing, which is a non-ductile failure mode.

It is possible to change this failure mode by:

1. Reducing the compression stress in the columns...
 - a) ... by reducing the vertical load (see.)
 - b) ... by increasing the columns r.c. cross-section
 - c) ... by increasing the column capacity using steel bracketing
 - d) ... by changing the load path so as to unload the most compressed columns.
2. Increasing the compressive strength of the concrete, therefore forcing reinforcement to yield before concrete crushes.
3. Decreasing the yield capacity of the reinforcement.

The other options of strengthening should be confined in the limitations of d_{lim} .

In these conditions the intervention method has to increase the lateral stiffness of the structure. If the lateral stiffness remains the same and the capacity increases, the value of d_{lim} starts to govern the design. This method can not successfully solve the problem of the structure, because the deformation can not increase above d_{lim} , while the elastic strength will not reach the level of required base shear.

On the other hand, the decreasing of the stiffness will evidently result in unsatisfactory performance, because the frame will reach the limit displacement d_{lim} , following almost immediately an elastic response path. The failure would become sudden, by crushing of concrete fibers in some column.

9.1 Rehabilitation using LGS shear walls

The stiffening of the frame by LGS walls will also result in an increase of the force demand as the structure is shifted in the lower period range of the spectrum. With the deformation capacity of the frame limited to d_{lim} , and the necessity to stiffen the structure, it is clear that the design will be primarily based on strength and less on ductility.

The increase of stiffness can be achieved by one the schemes presented in Figure 19. From the theoretical point of view there is no significant difference between the two schemes. In practices scheme (a) is more feasible.

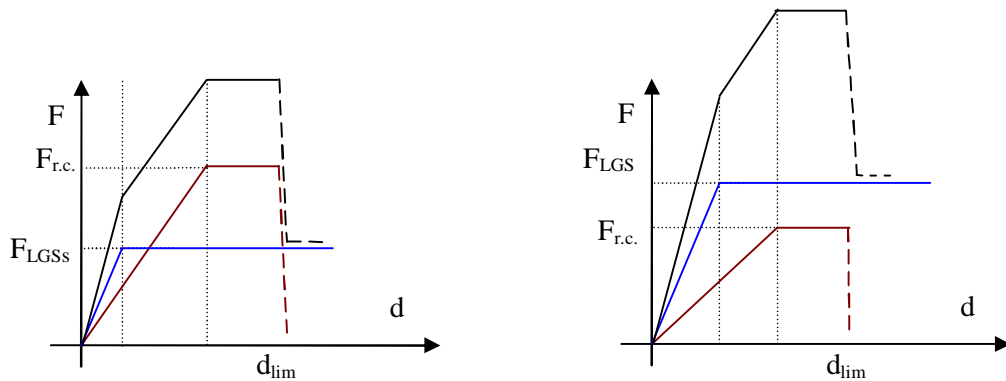


Figure 19. Suggested use of the LGS steel shear walls.

9.1.1 Properties of LGS steel plates used for rehabilitation

For the evaluation of the stiffness and strength of a steel plate with the dimensions of $L_{plate} \times H_{plate}$, welded to a rigid frame on all margins, the formulas proposed in [8] will be used.

The method supposes that the thin steel plate acts in tension alone, and the welded case obviously refers to an upper bound in terms of rigidity and strength supply of the plate. The consequence of using bolted connections instead of welds is a significant reduction of both stiffness and strength.

In [8] the following simplified formulas are proposed:

$$F_{plate} = \frac{1}{2} \cdot t_{plate} \cdot f_y \cdot 2 \cdot L_{plate} \cdot \sin(2 \cdot \alpha) \quad (5)$$

$$K_{plate} = \frac{1}{4} \cdot \frac{E \cdot t_{plate} \cdot L_{plate}}{H_{plate}} \cdot \sin^2(2 \cdot \alpha) \quad (6)$$

Where t_{plate} is the thickness of the plate
 f_y the yield stress of the plate
 E the elastic modulus of the plate material (steel)
 α the inclination angle of the yield stress developing in the steel plate, when the frame is subjected to shear. The value this angle can be evaluated using the Eq. 7 (H , $2 \cdot L$, t in mm):

$$\alpha_{DEG} = 45 - (0.0035 \cdot t_{plate} + 0.00263) \cdot (H_{plate} - L_{plate}) \quad (7)$$

9.1.2 Performance of the strengthened structures

In the two main directions of the structure, the steel plates were used in the bays presented in Figure 21a and b. The first arrangement is idealized, as very often architectural considerations will impede the use of such symmetrical strengthening scheme. As principle, the shear walls should be placed (i) as symmetrically as possible in both directions and (ii) as close to the outer frames as possible, in order to increase resistance to torsion.

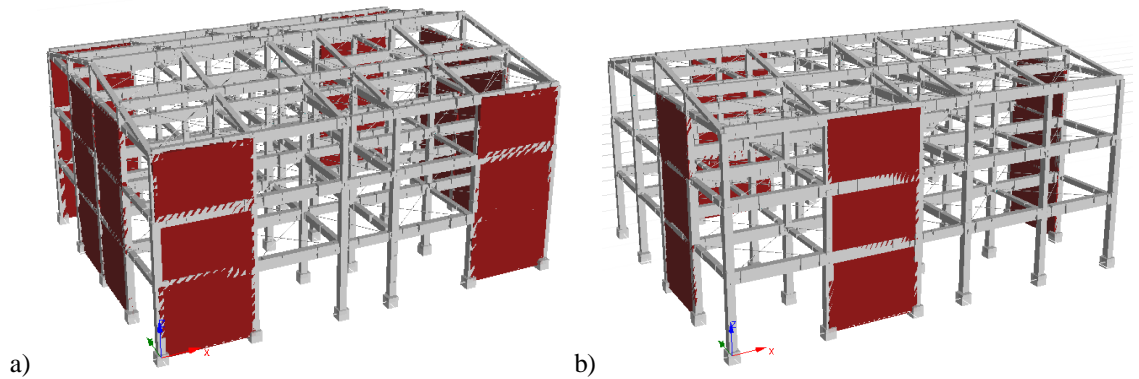


Figure 20. Possible strengthening with LGS shear walls (a) W1, (2) W2.

Several thicknesses of LGS shear walls have been tried in order to achieve an optimum performance for the structure. The results presented here refer to the LGS plate dimensions from Table 8.

Table 7. LGS shear walls in X and Y direction.

Dir.	Axis	L (m)	H Plates	H (m)	L (mm)	α (deg)	t (mm)	f_y (N/mm ²)	F_{plate} (kN)	K_{plate} (kN/m)	F_{wall} (kN)	K_{wall} (kN/m)
X	A & E	4.6	4	3.35	1150	38.6	1	350	392	34256	1570	137023
	Y	1&6	4.1	3	3.35	1367	41.2	1	350	474	42094	1423

The deformed shapes from the two direction pushover are present in Figure 22, while the capacity and demand diagrams are presented in Figure 23 for this rehabilitation case. The numerical values of the same cases are presented in Table 10. It can be observed that the soft storey behavior of the ground floor is preserved in this case.

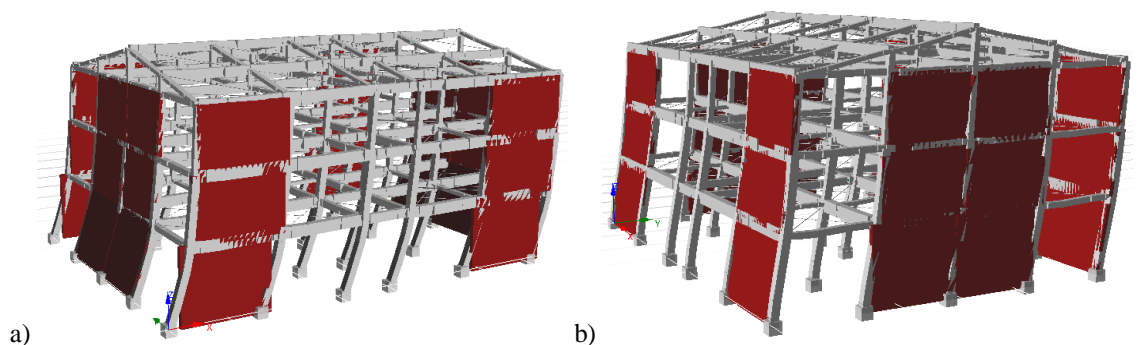


Figure 21. Deformed shape before failure from pushover in (a) X and (b) Y directions.

As it can be seen, the strength of the structure increases in both direction so that the ductility requirements are very low ($\mu_{\text{req-x}} = 2.78$, $\mu_{\text{req-y}} = 2.78$). The LGS walls, together with the RC frame provide sufficient strength almost for an elastic response; and the strength is enough for a design with $q = 1.5$.

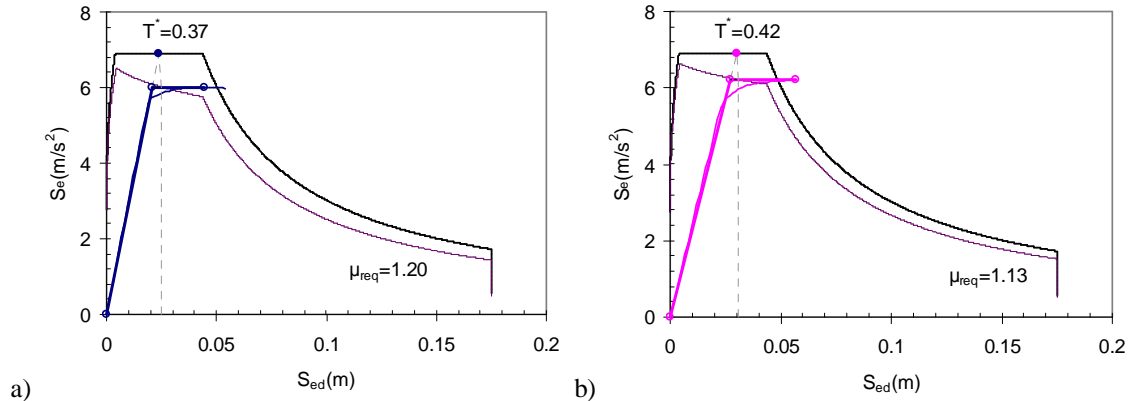


Figure 22. Demand and capacity diagram of the equivalent SDOF system (Annex B, EN 1998).

It is important to note that in this case of modeling, the shear walls are modeled as simple shear links between the two levels they connect. This means that shear walls are connected to the frames only in the corner, and local forces exercised on RC elements are not taken into account. The most important of these local effects are: (i) the anchoring of the shear wall to the RC elements and (ii) the uplift effect of the wall on the foundation on the tension side.

In order to account for the local effects of the LGS shear walls, a more elaborate model was developed where strips play the role of shear wall (). Several simplifications are accepted in this case of modeling too: (i) the strips are made of bi-linear yielding steel material, (ii) they are very thin, $t = 1$ mm, and they can act only in tension, (iii) i.e. they are meant to model the tension field effect in a very thin steel plate, so shear and compression are neglected, (iv) strips are placed at an angle of 45° , so the presumed tension field is forced to develop at this angle. This is not always the case, as the tension field in a thin steel plate develops under an angle depending on the dimensions of the plate (i.e. as in Eq. 7).

In these models, at the base of the shear plates has been connected to a IPE500 base girders, which are supplementary placed between the columns. This model is similar to the one in Figure 20b, so results from the two will be presented together.

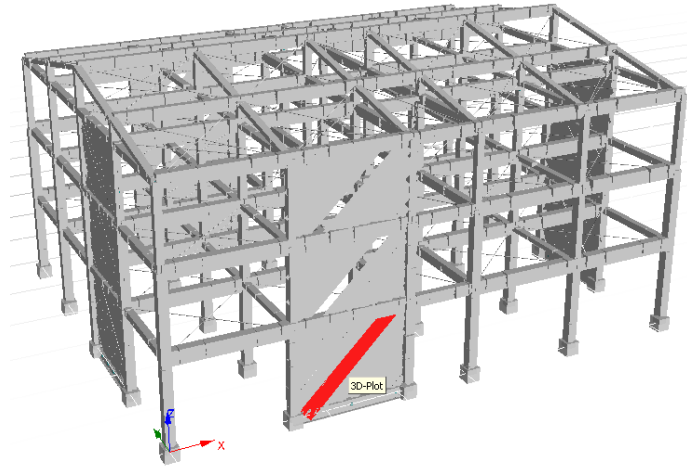


Figure 23. Modeling the LGS shear walls as inclined strips (W2-Strips).

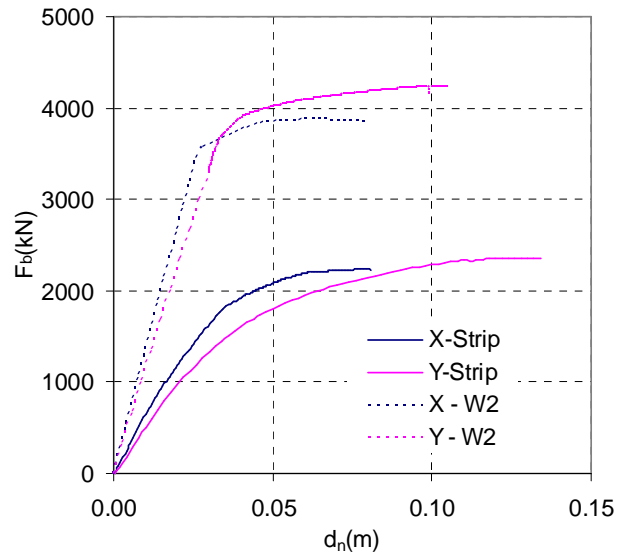


Figure 24. Pushover curves of the W2 and W2-Strips configurations.

As it can be observed in Figure 24, the modeling of the shear walls as an equivalent shear element between the floor levels gives a very conservative estimate of the strength and stiffness. This happens because the formulations presented in Chapter 9.1.1 are based on the supposition that the frame bordering the LGS wall is perfectly rigid and full-strength. However, the deformations of the RC elements also contribute to the overall displacement, limiting the effectiveness of the LGS wall. Even with the modeling of the LGS wall as strips, several concerns remain, as: (i) it is supposed that strips do not fail at end connections and (ii) the transverse compression (and consequent buckling) of the LGS plate can lead to the formation of important local stress concentrations, and high strains that can further reduce the capacity of the LGS wall.

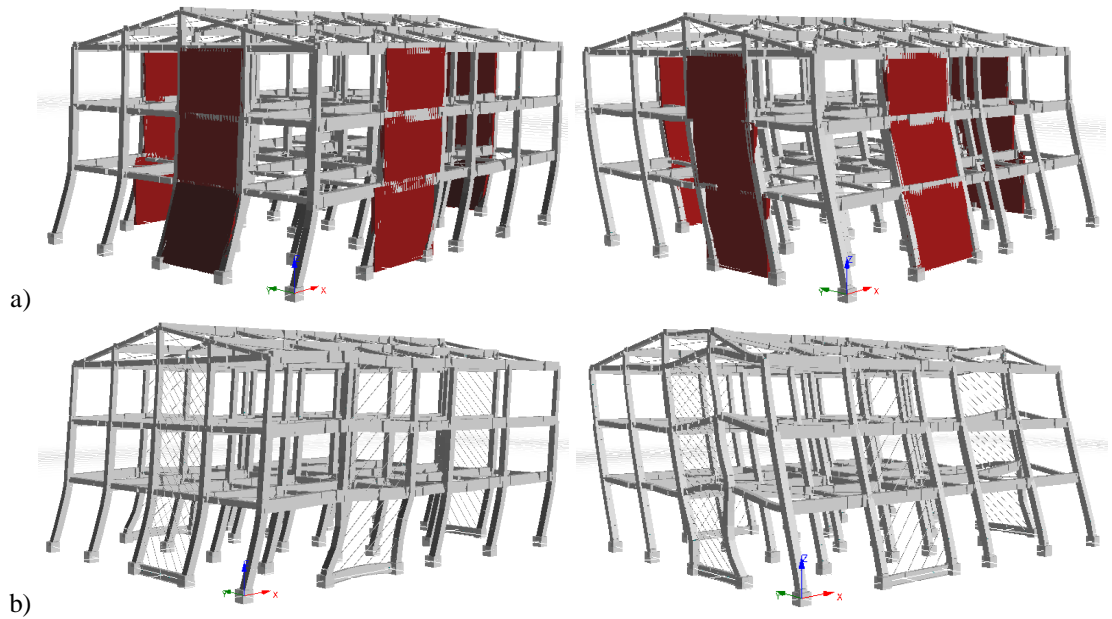


Figure 25. Deformed shapes under pushover for the (a) W2 and (b) W2-Strips configurations.

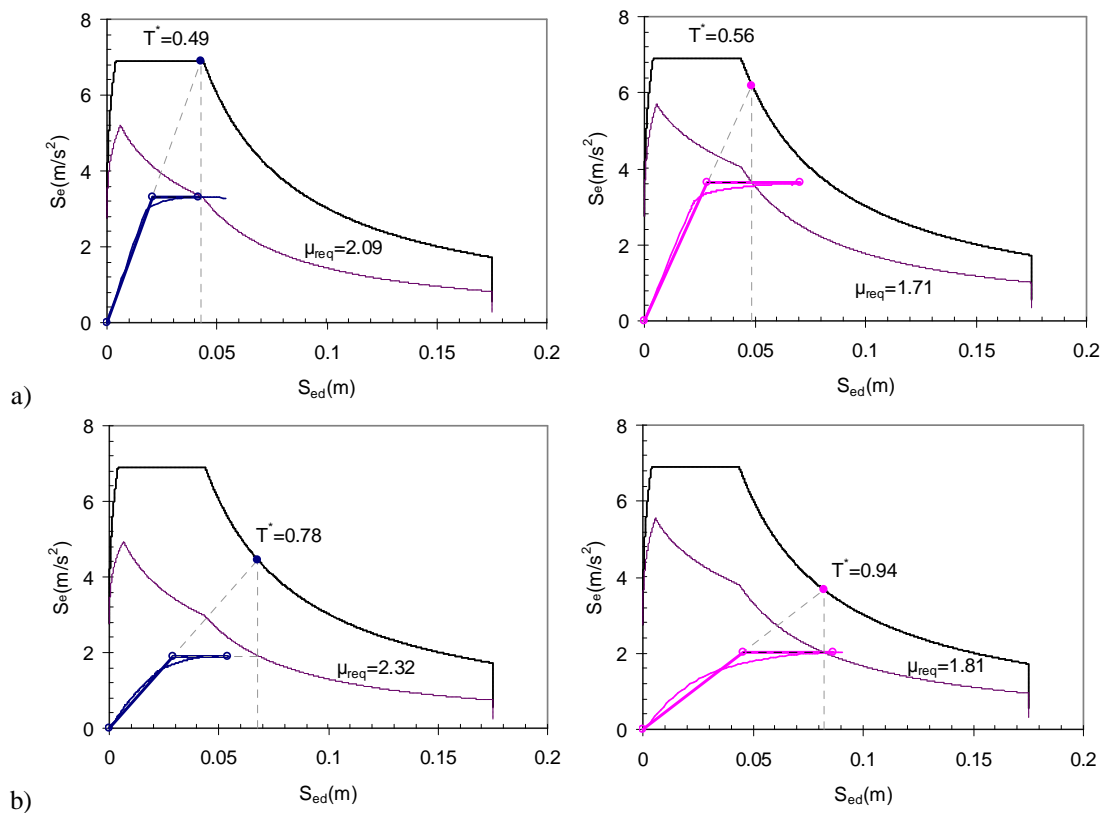


Figure 26. Demand and capacity diagram of the equivalent SDOF system (Annex B, EN 1998): (a) X and Y direction of the W2 model, (b) X and Y direction of the W2-strip model.

9.2 Rehabilitation by reducing the mass

As mentioned, one method to rehabilitate the structure would be to make it lighter. The solution of replacing the roof with a LGS trapezoidal sheeting, and replacing the walls with LGS walls (e.g. NORDICON walls) is examined in the

following section. If the self-weight of the new LGS elements is presumed to be 25 kg/m^2 (i.e. down from 200 daN/m^2 for roof, and 250 daN/m^2 for walls), the structures mass is reduced in the EQ combination from 1357.6 t to 1112.7 t . The new distribution of the masses and horizontal loads is summarized in Table 8.

Table 8. Distribution of the horizontal loads in the 3D structure.

	Level	$m_i(\text{t})$	$h_i(\text{m})$	Φ_i	$m_i \times \Phi_i$	$m_i \times \Phi_i^2$	$h_i \times m_i \times \Phi_i$	F(%) / Level
X or Y direction	1	410.8	3.9	0.31	128.7	40.3	501.8	20.5
	2	400.6	7.3	0.59	234.9	137.7	1714.7	37.4
	3	238.3	10.65	0.86	203.8	174.4	2170.9	32.5
		40.8	11.55	0.93	37.9	35.1	437.3	6.0
	Roof	22.2	12.45	1	22.2	22.2	276.7	3.5
	Total:	1112.7			627.5	409.8	5101.5	100.0

The capacity and demand curves for this case are presented in Figure 27. It is clear that this solution can not improve the performance to the desired level. Summary of the data from Figure 27 is also in Table 8.

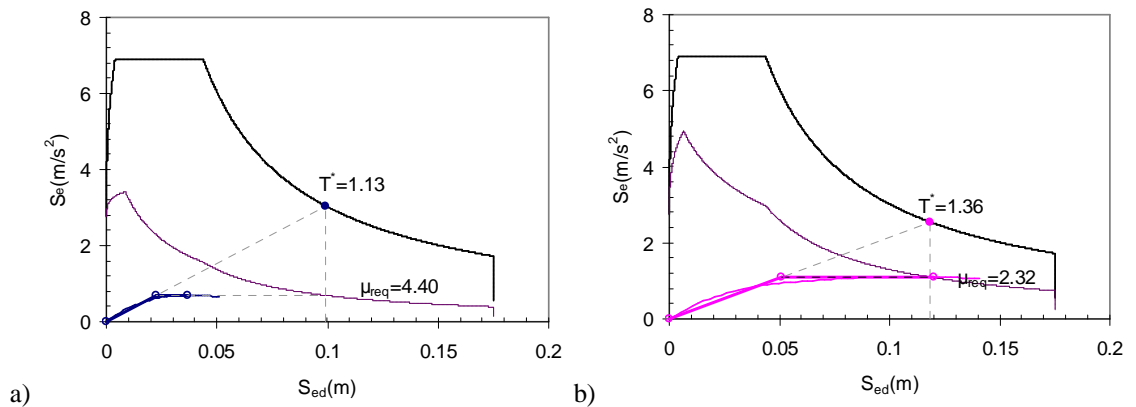


Figure 27. Capacity & demand of structure with LGS wall & roof.

9.3 Rehabilitation by confining the concrete in critical areas

In this structural configuration, it was supposed that certain elements of the structure will be confined using FRP bandaging, therefore providing increased ductility and strength in these regions. An increase of 80% strength has been presumed in the confined regions; the compressive strength of the concrete being supposed to increase to $R_{ck} = 36 \text{ MPa}$, while the strain at maximum stress was unchanged $\varepsilon_{u,N} = 0.002$.

The region was supposed to extend only to selected columns in the original structures. All ground floor columns have been confined on a 1m height both at the top and at the bottom. Further, columns on the first floor at axes A1, A3, A4, A6, B1, B3, B4, B6, C1, C3, C4, C6, D1, D3, D4, D6, E1, E3, E4, E6 (see [3] for the geometry of the building), have been confined on an interval of 1m at the bottom. This effectively means that the base of the structure has been strengthened, together with the region of the first floor.

However, this confinement scheme has not changed the deformed shape of the structure under pushover loading. In fact, the deformations remained identical to the ones presented in Figure 12. The pushover curves, however, underwent slight modifications, in the sense that significant ductility has been gained. The improvements can be observed by comparing Figure 28, presenting the pushover curves of the confined frame, to Figure 16 corresponding to the initial frame. As it can be observed, the improvements are more significant in the Y direction; mostly because in the X direction the plastic deformations are still entirely concentrated at the ends of the columns on the ground floor. Based on the curves in Figure 28, it can be said that the confined structure marginally fulfills the earthquake design requirements in the Y direction; but it is inadequate in the X direction.

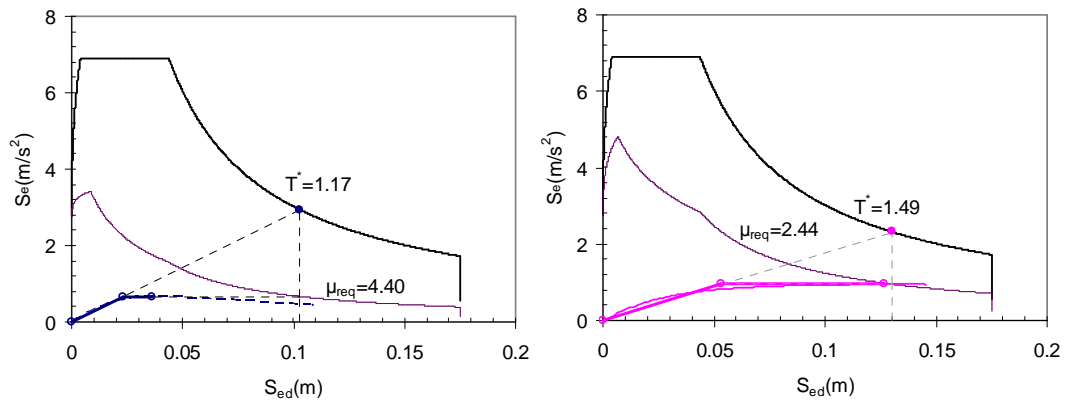


Figure 28. Capacity & demand of structure column confined column ends.

9.4 Rehabilitation by changing the column cross-section

The idea of this rehabilitation is to improve the performance by increasing the cross-section of the most loaded columns. Additional reinforcement has been added by using LGS corner profiles (i.e. some sort of bracketing), and the r.c. core of columns has been increased to cover the newly added steel (Figure 29). Only the columns of 40 x 40 cm have been changed, affecting all columns on the ground floor, and about half on the 1st floor.

The confining effect on the existing concrete and the change of mass has been ignored in the analysis.

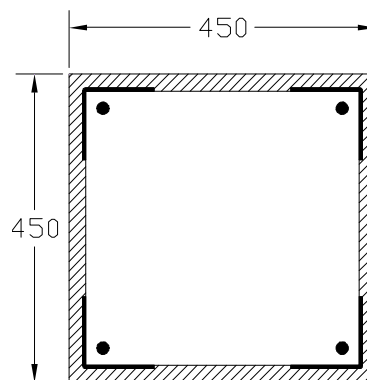


Figure 29. Initial (a) and increased (c) cross-section of column type Coll.

The demand and capacity curves of this configuration are presented in Figure 30, while the pushover deformed shapes in Figure 31.

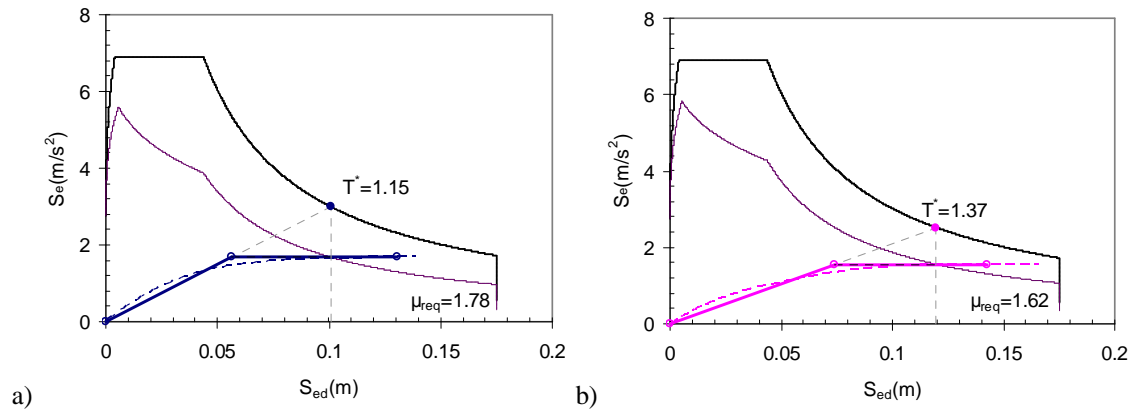


Figure 30. Capacity & demand of structure bracketed columns.

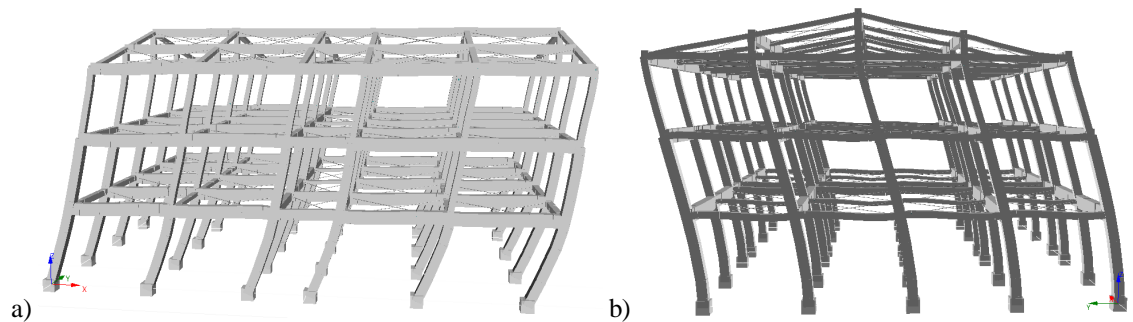


Figure 31. Pushover deformations in X (a) and (b) Y directions.

As it can be observed on the deformation shapes, in the X direction, the columns became stronger than the beams. The plastic deformations are concentrated now in the beam ends. This is advantageous. In Y direction, the plastic hinges are clearly formed only at beam ends (Figure 31b), columns being elastic.

In both directions, just before the drop of the base shear, the crushing of the concrete fibers took place at some beam ends. This suggests that even if the columns are further strengthened the capacity of the frames can not be increased.

9.5 Summary of the possible rehabilitation procedures

A summary of all suggested rehabilitation procedures is presented in Table 9. The properties presented there are the ones corresponding to the equivalent SDOF system. The main parameters of the different configurations are also highlighted in the table.

Table 9. Summary of the properties of the equivalent SDOF (Annex B, EN1998-1-1) in all strengthening cases.

	Initial RC frame		LGS wall (W2 Strip)		Mass reduction/ Light roofs & walls		Concrete confinement		Bracketed Column	
	X	Y	X	Y	X	Y	X	Y	X	Y
d_{\max}^* (m)	0.039	0.100	0.054	0.086	0.037	0.120	0.036	0.127	0.131	0.143
F_{\max}^* (kN)	490	717	1507	1591	434	687	526	749	1323	1229
d_y^* (m)	13.1	52.6	59.2	101.1	11.0	65.0	13.0	74.9	135.4	130.1
T^* (s)	1.25	1.51	0.78	0.94	1.13	1.36	1.17	1.49	1.15	1.37
S_{e-T^*} (m/s ²)	2.76	2.29	4.45	3.66	3.05	2.55	2.94	2.32	2.99	2.52
S_{ed-T^*} (m/s ²)	0.110	0.132	0.068	0.082	0.099	0.119	0.103	0.130	0.101	0.120
q_u^*	4.44	2.51	2.33	1.82	4.41	2.33	4.41	2.44	1.78	1.62
d_t^* (m)	0.110	0.132	0.068	0.082	0.099	0.119	0.103	0.130	0.101	0.120
μ_{req}	4.43	2.51	2.32	1.82	4.40	2.32	4.41	2.44	1.78	1.62
μ_{ava}	1.58	1.90	1.84	1.90	1.63	2.35	1.56	2.37	2.31	1.93
d_t (m)	0.163	0.196	0.101	0.122	0.152	0.182	0.152	0.193	0.150	0.178

In essence, when comparing the different cases, one should concentrate on the base shear force capacity (F_{\max}^*), the period of vibration (T^*), the required (μ_{req}) and available ductility (μ_{ava}). In principal, when the available ductility is larger than the required one, the structure fulfills the ULS designed requirements for the given earthquake loads ($a_g = 0.23 \times g$, see §8.2). Supplementary, one should also follow the variation of the period of vibration, as a very high value may indicate excessive flexibility of the structure; in which case the SLS design criteria will not be met.

As discussed in the previous chapters, the initial R.C. frame is very flexible in both directions ($T_x^* = 1.25$ s, $T_y^* = 1.51$ s). Also, the lack of available ductility in both directions can be seen.

The first rehabilitated frame, using LGS shear walls, is both stiffer ($T_x^* = 0.78$ s, $T_y^* = 0.94$ s) and stronger ($F_{\max_X}^* = 1507$ kN, $F_{\max_Y}^* = 1591$ kN) than the origin frame. The level of the required ductility is compatible with the available ductility in both directions (Table 9). With some modifications, the LGS shear wall solution can lead to a satisfactory design.

As it can be observed (Table 9) both reducing the mass and confining columns proved to be insufficient to fulfill earthquake criteria. Especially in the X direction, the levels of the ductility provided by these configurations, is completely inadequate.

Finally, the LGS bracketed column solution is also a promising alternative, from the ULS point of view. As it can be observed, the ductility levels are adequate. The only concern with this configuration is that the periods of vibration remain rather high; it might be that difficulties arise in fulfilling SLS requirements (i.e. this has not explicitly been investigated).

An overall assessment of the deficiencies of the R.C. frame, together with a performance comparison of the proposed intervention methods, is presented in Table 10. A number of nine deficiencies of the initial structure have been identified in the table; together with the main direct cause of the deficiency.

The applied intervention techniques are than listed; specifying if it is the objective of the specific techniques to correct some of the deficiencies. E.g. the LGS shear wall intervention had the aim of: eliminating the weakness of the frame in the X and Y direction, and (ii) to increase the torsion resistance of the structure. It can be read from the table that, this intervention technique has mostly reached its goals and it is declared a potential solution for the rehabilitation. On the other hand the “concrete confinement” intervention had the goal to increased ductility of the frames in both directions. As it is mentioned in Table 10, this technique has not achieved its goal, and was declared overall inefficient for the rehabilitation of the frame.

Table 10. Comparative performance of the rehabilitation methods.

Nr.	Problem	Cause	LGS walls		Intervention technique					
			Obj.	?	Mass reduction Obj.	?	Concrete confinement Obj.	?	Column bracketing Obj.	?
1	Weak in X direction;		Main	Yes	-	-	-	-	Yes	Yes
2	Weak in Y direction;	Beams are weak	Main	Yes	-	-	-	-	Yes	Yes
3	Flexible in X direction $T_x^* = 1.25$ s;	Columns are weak	Main	No	Yes	No	-	-	Yes	No
4	Flexible in Y direction $T_y^* = 1.51$ s are quite large;	Beams are weak	Main	No	Yes	No	-	-	Yes	No
5	Not ductile enough in X direction	Because failure is local in the 1 st floor	-	-	-	-	Main	No	Yes	No
6	Not ductile enough in Y direction		-	-	-	-	Main	No	Yes	No
7	X direction sudden crushing/failure	Existing level of compression force on some columns	-	-	Main	No	-	-	Main	Yes
8	In the X direction the structure is weak-column/strong-beam;		-	-	-	-	-	-	Main	Yes
9	Possible that the frame is torsion sensitive ($T_{Tors} \sim T_{Xtrans}$);		Yes	-	-	-	-	-	-	-
OVERALL ASSESEMENT			OK		Failure		Failure		OK	

10 Performance based (PBD) interpretation of the results

One of the goals of this analysis is to discuss, both the performance of the initial frame and that of the rehabilitated frames, within the context of performance

based design (PBD). In other words, based on the performed analysis, it is desirable to determine the performance limits of the frames before, and after rehabilitation.

If in the following section, the pushover curves from the initial r.c. frame and from the LGS shear wall strengthened frame are interpreted in PBD terms. The process is described below:

STEP 1: The initial data is the pushover curve of the frame (1) in a certain direction and (2) presuming a given distribution of horizontal loads (i.e. in this document triangular). The curve in this stage refers to the structure, and it is base shear force vs. structural displacement format.

STEP2: The pushover curve is transformed in PSA/SD format using the procedure described e.g. in Annex B of EN 1998-1 [4]. The obtained curve refers already to the equivalent SDOF of the structure.

STEP3: The non-linear curve is synthesized in an equivalent elastic-plastic (EP) curve. E.g. the same Annex B [4] provides a procedure of transformation from the non-linear curve to the idealized EP behavior. The assumption in the Annex B procedure is that the yield force of the SDOF is equal to the ultimate strength. I.e. the point corresponding to the largest force on the curve is the ULS point in the behavior. The decreasing branch of the non-linear is disregarded, and all equivalent EP properties (e.g. stiffness, yield displacement, ductility, etc.) are determined using this point as ULS point. This method has been used in this document (see Figure 15), but it should be noted that there is no universal definition of how to obtain equivalent EP behavior from a non-linear curve.

Other transformation methods follow the decreasing branch of the pushover curve up to a loss of capacity of 10 or 20%, and use this point as ULS point for the behavior. For proper application of the PBD procedure, other performance levels should also be defined, based on the initial pushover curve.

STEP4: Knowing the available ductility (μ_{ava}) in the ULS stage from the equivalent EP curve; an elastic and an inelastic spectrum, corresponding to μ_{ava} , can be plotted in a PSA/SD format, so that the EP curve and the inelastic spectra just intersect.

STEP5: The PGA (a_g) for this two spectra was drawn corresponds to (1) the ULS performance limit of the frame, (2) in the given direction and (3) presuming a given distribution of the horizontal forces. The PGA corresponds to ULS, because the EP curves end is accepted as ULS point in the behavior; and it refers to the direction and horizontal force distribution for which the pushover curve was generated and the equivalent SDOF transformation was carried out.

The above procedure was applied to the initial r.c. frame using both X and Y direction pushover curves. The results are presented in Figure 32a. The two EP curves in Figure 32a are reproductions of the ones in Figure 16, and are based on values summarized in Table 9. As it can be observed, the available ductility of the initial structure was $\mu_x = 1.58$ and $\mu_y = 1.90$ at ULS. The available base shear capacity was also larger in the Y than in the X direction, but this is of secondary importance. The two pairs of spectra in Figure 32a are: (1) with full lines, elastic spectra corresponding to $a_{gx} = 0.08$ g (with blue for X direction) and to $a_{gy} = 0.17$

g (with magenta for Y direction) and (2) inelastic spectra (with dotted lines), created from the above elastic spectra using ULS ductility of $\mu_x = 1.58$ and $\mu_y = 1.90$ in the two loading directions.

As it can be observed, the EP lines are just intersecting the non-linear spectra. The intersection points are the ULS performance point of the initial r.c. frame in the X and Y directions. In other words, the initial r.c. frames ULS performance corresponds to earthquakes with $a_{gx} = 0.08$ g in the X, and $a_{gy} = 0.17$ g in Y direction.

As it can be observed from Figure 32b, the use of the LGS shear wall strengthening procedure improves the performance of the frame in both directions. The new values of the PGA corresponding to ULS are $a_{gx} = 0.18$ g and $a_{gy} = 0.24$ g.

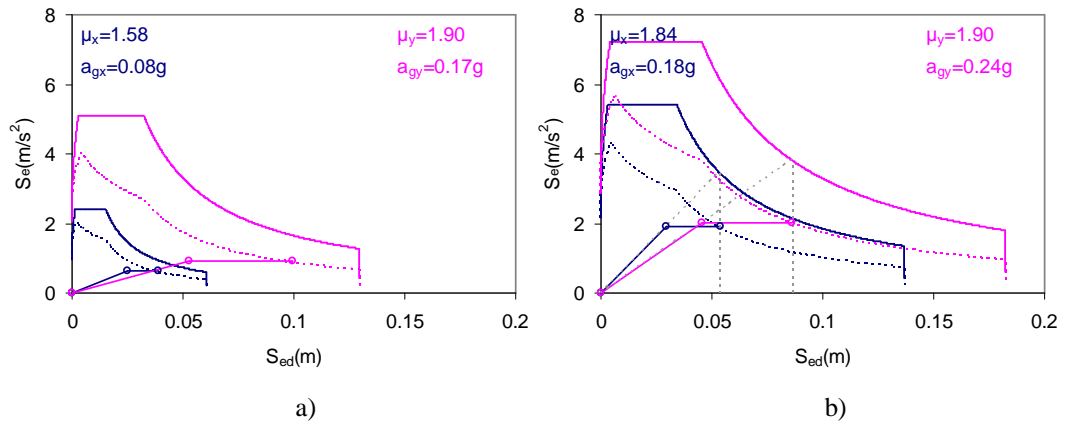




Figure 32. ULS performance points for the (a) initial structure and (b) the one strengthened with LGS shear walls.

Using the above curves the PGA levels corresponding Life Safety/ULS performance can be presented in the building performance objective table accepted in the earlier STEELRETRO report [9]. In Table 11 and Table 12, the return periods (MRI) are as agreed in [9], based on Eurocode 8 and the Italian code D.M.2008. The PGA values are determined based on the agreed methodology in [10].

Table 11. PBD table of the effect of the upgrade with LGS shear walls (D.M.2008).

	Italian Code for construction (D.M.2008)	PGA/ a_g (g)	Performance level		
			IO	LS (ULS)	CP
Earthquake Hazard Level	Occasional - MRI = 50 years	0.094		~INI	↻
	Rare - MRI = 475 years	0.23		~LGS	
	Very Rare - MRI = 975 years	0.292			

Table 12. PBD table of the effect of the upgrade with LGS shear walls (Eurocode 8).

	Italian Code for construction (D.M.2008)	PGA/a _g (g)	Performance level		
			IO	LS (ULS)	CP
Earthquake Hazard Level		0.08		~INI	
	Occasional - MRI = 225 years	0.176		~LGS	
	Rare - MRI = 475 years	0.23			
	Very Rare - MRI = 2475 years	0.39			

Note: IO - Immediate Occupancy; LS - Life Safety; CP - Collapse Prevention

As it can be observed, according to the Italian D.M.2008, the initial structure is substandard for the Life Safe performance level. With the LGS shear wall upgrade, the required PGA = 0.23 g level is not reached; but with some more adjustments in the X direction it is clearly within reach.

According to the EN1998-1-8 criteria, the initial building is extremely deficient. Even after the LGS upgrade, the hazard level corresponding to occasional earthquakes is barely surpassed. As it can be observed in Table 12, the EN1998 hazard levels are problematic in the sense that “Occasional” and “Rare” earthquake levels are very close to each other. Therefore the building has to fulfill the immediate occupancy and life safety criteria for almost the same PGA levels.

11 Conclusion

The initial r.c. structure has several potential weaknesses in an eventual earthquake loading scenario:

- The stiffness is reduced in both directions, resulting in exaggerated vibration periods (1.25 s, 1.51 s). If it is accounted that the concrete is in partially cracked state, the vibration periods would be even higher;
- Strength is insufficient in both directions, resulting in large ductility demands (i.e. ductility factors 4.5 and 2.5);
- Ductility is very limited in both directions, mostly because columns are loaded with high axial forces. In all cases, the failure during the pushover process occurred by crushing of the compressed concrete in some columns. In fact this phenomenon is limiting the ability of the structure to deform laterally in the non-linear range;
- In the X direction, the structure is a weak column strong beam structure, vulnerable to forming storey mechanisms.

After identifying these structural problems several methods to rehabilitate the structure have been tried.

- ... by using LGS shear walls;
- ... by making the structure lighter using LGS external walls and roofs;
- ... by confining ground floor columns in order to increase their strength and ductility;

- ... by bracketing the columns of the structure in order to increase bending strength and the ability to sustain plastic hinge rotations.

It has been shown that only two of the above: (1) the LGS walls and the (2) column bracketing, has the potential to significantly improve the performance. The rehabilitation based on LGS walls strengthens and stiffens the structure. The period of vibration is significantly reduced, and the ductility is increased. The column bracketing solution leaves the stiffness unchanged, while increasing strength and ductility.

It should be noted that only ULS design checks have been performed for the frames; it is very likely that column bracketing leaves the structure too flexible to fulfill the SLS design criteria. Based on this observation, it is suggested that structure can be retrofitted to satisfy earthquake design criteria only by using stiff horizontal load bearing systems (e.g. shear walls).

References

- [1] Eurocode 1: Basis of design and actions on structures, Part 2-1: Densities, self-weight and imposed loads, European Committee for Standardization, Brussels.
- [2] prEN1990. "Eurocode - Basis of structural design." Brussels: European Committee for Standardization, 2001.
- [3] Braconi A., Osta A., Nardini L., Salvatore W., (2008) WP 3,4,5 and 6: Cost, performance and constructive analysis of steel solutions for retrofitting vertical elements, floors, roofs and foundations; definition of the reinforced concrete benchmark building for the execution of comparative performance analysis between steel intervention techniques, PRECSATEEL 10.05.2008 draft for discussion.
- [4] EN1998-1. "Eurocode 8: Design of structures for earthquake resistance. Part 1: General rules, seismic actions and rules for buildings." Brussels: European Committee for Standardization, 2005.
- [5] SEISMOSTRUCT Help system.
- [6] Chopra A. K., Goel R. K. "Capacity-demand-diagram Method for Estimating Seismic Deformation of Inelastic Structures: SDF Systems." Berkeley: Pacific Earthquake Engineering Research Centre, 1999.
- [7] Chopra A.K., "Dynamics of Structures, Theory and applications to earthquake engineering." Prentice-Hall, 2008. (§13.1.2 - Modal expansion of displacements and forces).
- [8] Fulop L.A., Hakola I., Design method for light-gauge steel shear walls sheathed with flat steel plates, Advanced Steel Construction Vol. 3, No. 3, 2007 (p. 628 - 651).

- [9] Bonessio, Noemi, Bordea, S., Braconi, A., Braga.,F., Dogariu, D., Dubina, D., Lomiento, G., Osta, A., Salvatore, W., and Stratan, A. "Six-Monthly Report: STEEL SOLUTIONS FOR SEISMIC RETROFIT AND UPGRADE OF EXISTING CONSTRUCTIONS." RIVA Acciaio S.p.A., 2008.
- [10] Minutes of STELRETRO meeting. 6-7 Sept. 2008, Timisoara.